Astron. Astrophys. 152, 130–150 (1985)

ASTRONOMY AND ASTROPHYSICS

Time dependent chemistry in dense molecular clouds

I. Grain surface reactions, gas/grain interactions and infrared spectroscopy

L.B. d'Hendecourt [1,2], L.J. Allamandola [1,3], and J.M. Greenberg [1]

[1] Laboratory Astrophysics, Huygens Laboratorium, Wassenaarseweg 78, NL-2300 RA Leiden, The Netherlands
[2] Groupe de Physique des Solides de l'ENS, T23, 4 Place Jussieu, F-75251 Paris Cedex 05, France
[3] NRC Senior Associate, NASA Ames Research Center, Mail Stop 245/6, Moffett Field, CA 94035, USA

Received June 21, 1984; accepted May 21, 1985

Summary. We have developed a model which examines the continuous interaction between grain surface processes with an ion-molecule gas phase chemistry scheme. Considering only a limited but realistic grain surface scheme including accretion, surface migration, reactions and ejection, it has been possible to follow the effects of accretion of gas phase species on grain mantle evolution. Reaction driven ejection of molecules from the mantles back to the gas phase is described. The ejected molecules modify the gas phase abundances and also participate in the gas chemistry for which 551 individual reactions involving 73 chemical species are computed time dependently. The main results show that:

i) Complete accretion is prevented and while equilibrium between the gas and the grains is reached, their respective compositions differ markedly.

ii) At short timescales, abundant production of H_2O, CH_4, and NH_3 is due entirely to grain surface reactions. The CO molecule is made in the gas phase.

iii) Grain mantle composition shows strong time dependence because of the gradual conversion of atomic to molecular hydrogen and atomic carbon to carbon monoxide in the gas.

iv) Due to efficient neutralization at the surface of negatively charged grains, metal abundances do not play a crucial role on the electron and molecule abundances.

v) The abundance of molecules like H_2O, CH_4, and NH_3, made efficiently on the grains at short times, decreases at longer times; CO, CO_2, O_2, N_2 and, in some cases, H_2O eventually dominate the composition of the grain mantle at longer times.

vi) H_2O rich mantles are expected for low to moderate values of extinction. O_2/CO rich mantles are obtained for high UV extinction when molecular oxygen dominates the gas phase. A comparison between calculated and observed gas phase abundances is made and infrared spectra of the calculated grain mantles are compared with interstellar dust absorption bands. Modification of the mantles, with emphasis upon UV photolysis, based on laboratory experiments, will be discussed in Paper II.

Send offprint requests to: L.B. d'Hendecourt

Key words: interstellar medium: dust – molecules

1. Introduction

Since the first detection of simple, diatomic, interstellar radicals and ions in the 1930's and 40's, followed much later by the radio detection of OH and the identification of polyatomic molecules such as NH_3 and H_2CO, models of interstellar chemistry have grown considerably in complexity and sophistication. At present these models rely primarily on gas phase chemistry for which fast ion – molecule reactions play the dominant role. A considerable amount of work has been done which concentrates on the two different domains: the diffuse medium – where UV photodissociation is the dominant mechanism for the destruction of molecules (Black and Dalgarno, 1973, 1977) and the dense cloud medium – where cosmic ray ionization dominates and UV photodestruction processes can be largely neglected (Herbst and Klemperer, 1973). A review of the salient features of these different gas phase models can be found in Turner (1974), Gammon (1978), and Watson (1984).

The only molecule which is generally believed to form on grain surfaces is H_2 because it cannot be formed rapidly enough by a two-body (H + H) reaction in the gas phase without the help of a third body to dissipate the heat of reaction since radiative relaxation via vibration-rotation transitions is forbidden. Under interstellar density conditions, this third body can only be a grain (Hollenbach and Salpeter, 1970). Estimates of H_2 molecule formation rates in diffuse clouds agree well with this picture (Jura, 1974) and it should be noted that the H_2 molecule is required to initiate the rich gas phase chemistry which produces polyatomic molecules. Time dependent solutions of chemical reaction networks investigated by many authors have shown that starting conditions which include initially negligible molecular abundances must take the interaction of atomic hydrogen with grain surfaces into account to produce the molecular hydrogen required to begin molecular evolution (Graedel et al., 1982). Of course, if H can

reside on a surface long enough to react, all other atoms, radicals and molecules can interact on the grain surface as well.

Although time independent chemistry is often assumed, mainly for tractability, and certainly justified in the less dense medium by the relatively short timescales required to reach equilibrium in these clouds where photodestruction processes dominate (Black and Dalgarno, 1973; de Jong et al., 1980), several attempts to study the importance of time evolution of the gas phase chemistry in dense clouds have led to the conclusion that the equilibrium timescales are indeed rather long (of the order of 10^7 years) when compared to cloud lifetimes (Iglesias, 1977; Prasad and Huntress, 1980, and Graedel et al., 1982). In thise case, the accretion of heavy atoms, radicals and molecules on the ever present cold interstellar grains is inevitable and represents a dominant depletion mechanism for gas phase molecules. Iglesias (1977) has shown that, for an average density of $10^4\,cm^{-3}$, the accretion time is shorter than the time required for the gas to reach chemical equilibrium.

Surface chemistry had been suggested as a means to produce "dirty ice" mantles as early as 1949 by van de Hulst. Grain surface processes, leading to similar "dirty ice" mantles were later considered in detail by Watson and Salpeter (1972) who thoroughly reviewed the basic processes involved in grain surface chemistry and concluded that release mechanisms to the gas phase were simply too inefficient at these low temperatures to replenish the gas phase at the necessary rate. Surface chemistry involving purely thermodynamic driving forces for grain surface reactions has been considered by Allen and Robinson (1975, 1977) in order to compute the time dependent evolution of the gas phase from grain reactions alone. In this case, the grain mantle composition could not be inferred because this model invoked small grains (radius $<0.005\,\mu m$), implying direct ejection upon formation of the new molecule and no mantle production. This direct ejection process is not applicable to and does not prevent molecule formation on larger grains (radius $\gtrsim 0.01\,\mu m$). Recently, Tielens and Hagen (1982) calculated the mantle composition determined from the accretion of gaseous species using surface reactions with initial abundances calculated using an equilibrated gas-phase, ion-molecule reaction scheme. No feedback into the gas phase chemistry scheme was considered. Boland (1982) and Boland and de Jong (1982), computed gas phase and grain mantle composition from accretion, both with and without a more restricted set of surface reactions, again no feedback into the gas was considered.

Direct observational evidence in support of grain mantles has come about only recently. During the past 15 years, considerable improvements in observational techniques have been achieved in the middle infrared region of the spectrum (2–20 μm), the region where most molecular vibrations occur, and numerous spectra of infrared sources, many embedded in dense molecular clouds, have become available. These spectra provide a powerful tool, not only for the identification of interstellar molecules in both the gas and solid phase, but also for a general understanding of the physical and chemical conditions which prevail in dense clouds [e.g. Kessler and Phillips (1984), see chapters by Aitken and Roche, Allamandola, Willner and Scoville]. The presence of water ice was recognized quite early as giving rise to the 3.1 μm absorption band in objects such as BN, and is now believed to be in the amorphous form (Léger et al., 1979; Hagen et al., 1981). A considerable amount of laboratory work on different mixtures containing H_2O has been published in order to explain the width and peak position of the 3.07 μm band (Hagen et al., 1983). A more complete look at the spectra obtained from some of these imbedded sources (i.e. W33A) shows strong absorption features at 3.07, 4.6, 6.0, and 6.8 μm (Soifer et al., 1979), the bulk of which can be reproduced in the laboratory with "dirty ice" mixtures made of simple molecules such as H_2O, NH_3, CO and CH_3OH (Hagen et al., 1980). This work firmly established the presence of molecular ice mantles on interstellar grains in dense clouds. More recent observations of W33A and other protostellar objects have led to the positive identification of frozen carbon monoxide at 4.67 μm (Lacy et al., 1984) as well as the observation of another solid state feature at 4.62 μm which seems to imply the occurrence of energetic (UV?) processes which can modify the chemical composition of the mantle.

The observation of solid molecular mantles *and* gas phase species in dense molecular clouds implies that an efficient desorption mechanism is available to maintain an equilibrium between molecules in the gaseous and solid phases. This of course implies that feedback from the grains to the gas is important and should be studied. In parallel with the experiments undertaken at Leiden to identify interstellar infrared spectra, a study of several possible molecule ejection mechanisms has also been underway, with particular emphasis on investigating the theoretical predictions made by Greenberg and Yencha in 1973 who suggested that UV photolysis of molecular mantles at low temperatures could result in the formation and trapping of reactive free radicals within the mantles in sufficient quantity that, when triggered to react, they could drive the explosive evaporation of the mantle, producing an equilibrium between the gas and the solid phase. Experiments which successfully demonstrated this mechanism and the astrophysical implications have been described by d'Hendecourt et al. (1982). This provides a viable mechanism in which gas and solid state processes can be tied together. In conjunction with other advances in the understanding of low temperature solid state phenomena, this makes it now possible to model the processes which occur on grains and to study the influence grains have on the gas phase.

In this paper, the simultaneous time dependent chemistry of the gas and solid phases of interstellar clouds is treated. Gas and grains interact constantly via accretion and ejection and the abundances in the gas phase as well as in the mantle are presented. In Sect. 2, the method which has been used to carry out these computations is described. The gas phase chemistry, including the parameters used, is briefly summarized. Emphasis is put on describing the grain processes which are limited to a small number (18) of important and dominant chemical reactions which occur on cold (10 K), single sized (radius $\sim 0.1\,\mu m$) grains. The extreme complexity of possible surface reactions (Allen and Robinson, 1977) and the important uncertainties introduced when considering complicated reaction channels make it very unlikely that this type of approach will be tractable in regions where grains are warmer than, say, 50 K and processes which involve non-zero activation energies can occur. Ultraviolet photolysis processes are also difficult to incorporate because of the various possibilities introduced by the "in-situ" creation of hot atoms and other reactive intermediates when UV photons are absorbed in the mantle, making it possible for a reactant to overcome appreciable activation energy barriers. In this way, not only does the number of reactions, but also the number of reactants and products dramatically increase, making a simple computational simulation impossible. These effects however can be treated in a semi-empirical way, and the results from such an approach will be presented in a following paper, hereafter referred to as Paper II.

After describing the model in Sect. 2, results are presented in Sect. 3, where different reaction schemes and feedback effects are discussed. The sensitivity of these results to variations in density, extinction and elemental abundances is treated in Sect. 4. Apart

from presenting the abundances in the gas and in the dust, we focus on the relationship between the two phases and address questions such as: what modifications do grain processes cause in the gas phase chemistry? Are some particular molecules made abundantly on grains? Do the abundances of molecules in the solid phase reflect those in the gas phase? In Sect. 5, the results are compared with observations, including some discussion of the general infrared spectroscopic characteristics of the computed grain mantles.

2. The model

In this section the basic assumptions made and the parameters used in the calculations are discussed. We first present the gas phase chemistry, including a general discussion of the starting conditions e.g. abundances of the different elements and species, ionization rates due to primary cosmic rays, and temperature of the gas. Next, the interaction between the gas and the grains is treated which includes the accretion of electrons, ions, atoms, radicals and molecules onto the grains. The physical nature of the binding between these different species and the grain, binding energies, surface mobility and surface reactions are also discussed.

In this model, grain surfaces play an active role in the formation of different but simple molecules. Reactive species, e.g. atoms and radicals, can also reside beneath the surface becoming part of the mantle when covered by unreactive species such as saturated molecules. Bulk reactions i.e. diffusion controlled reactions inside the mantle, are not formally considered. However, chemical modification of the mantle by UV photoprocessing as well as possible cosmic-ray bombardment is likely to occur during the lifetime of a typical molecular cloud. These effects, considered in Paper II, are only briefly discussed here. Finally, release of molecules from the mantle of the grains back to the gas phase, via chemically driven explosive release, is discussed.

The main results of these computations are the abundances of the different molecules both in the gas as well as in the solid phase at different times during the life of a dense molecular cloud. Finally, it should be kept in mind that, because of computational compatibility requirements between the gas and the solid state scheme, it is not possible to make molecules in the solid which are different from those present in the gas phase. Thus, although species such as O_3, HO_2 and others are likely to be formed to some extent in the solid they are not taken into account here.

The time dependent solution of the set of differential equations describing the evolution of the chemical species is calculated using a variable order, variable step Gear method for a stiff system of first order ordinary differential equations (Hall and Watt, 1976). To provide a consistency check, equilibrium values obtained were compared with the results of Boland and de Jong (1982) for a similar set of input parameters. The equilibrium values calculated under these conditions fall within 10% of those published by Boland (1982) the difference being mainly due to the fact that we did not include their sophisticated treatment for H_2 and CO photodestruction.

2.1. *Gas phase chemistry*

The specific gas phase reaction network used has been adopted from de Jong et al. (1980) and Boland (1982) and is based on the ion-molecule reaction scheme of Herbst and Klemperer (1973) and Watson (1973). See Table A2 in Boland (1982) for a list of the gas phase reactions and rates used here. Although a more detailed reaction network, including more species and naturally more reactions is available in the literature (e.g. Prasad and Huntress, 1980), this more limited set was chosen because we are mainly interested in molecules containing the most abundant atoms H, O, C, and N. This restriction makes the problem of including grain related processes and the investigation of time dependent evolution tractable. The major modification to the Boland (1982) scheme is the introduction of metals in a way similar to that used by Prasad and Huntress (1980). The importance of metals has been emphasized by Oppenheimer and Dalgarno (1974), Guélin et al. (1982), and Graedel et al. (1982) for the role they play in determining both electron as well as molecule abundances.

In total, 551 gas phase reactions are included which involve the 73 molecules, radicals, atoms and ions listed in Table 1, made up of the 8 "species": e^-, H,He, O, C, N, Met, and G; where e^- represents the electrons, Met the metals, and G the grains. Here, as in virtually all gas phase reaction schemes, grains are actively involved only in the process of H_2 molecule formation by the recombination of two hydrogen atoms on the surface for which the rate given by Jura (1974) is adopted. The set of gas phase reactions used in these calculations includes ionization by primary cosmic-rays, ionization and destruction of molecules by UV photons, ion-molecule reactions and neutral-neutral reactions; metal involvement consists only of the photo-ionization, charge exchange, and electron recombination reactions which are listed in Table 2.

The photodestruction rate for H_2 has been neglected since only regions of dark clouds were considered where self-shielding effects are important and hence H_2 photodestruction is negligible (de Jong et al., 1980). The photodestruction rates for CO, H_2CO, CH_4, CO_2, O_2, and N_2 are taken from Mitchell et al. (1978) and the possibility of self absorption and shielding is neglected.

2.2. *Solid state processes*

In this section, the parameters relevant to the grain chemistry are discussed in the context of the following processes. First, the sticking of gas phase particles onto grains is examined. Second, the interaction between charged species and grains is considered in order to compute the resulting grain charge. Third, the problems associated with re-evaporation and mobility of atoms on the surface are discussed and finally the reaction scheme used to include the reactive role of the surface of the grain itself is presented. A distinction is made between species which are on the surface of the grain and hence, can have a certain mobility and react with other surface species, and those which are buried in the bulk of the grain mantle where their mobility is negligible and

Table 1. List of molecules, radicals and ions included in the reaction network

e^-, H, H^+, H_2, H_2^+, H_3^+, He, He^+, O, O^+, O_2, O_2^+, OH, OH^+, H_2O, H_2O^+, H_3O^+, C, C^+, CO, CO^+, HCO, HCO^+, H_2CO, H_2CO^+, H_3CO^+, CH, CH^+, CH_2, CH_2^+, CH_3, CH_3^+, CH_4, CH_4^+, CH_5^+, CO_2, HCO_2^+, C_2, C_2^+, C_2H, C_2H^+, C_2H_2, $C_2H_2^+$, $C_2H_3^+$, C_3^+, C_3H^+, N, N^+, N_2, N_2^+, NH, NH^+, NH_2, NH_2^+, NH_3, NH_3^+, NH_4^+, N_2H^+, CN, CN^+, HCN, HCN^+, H_2CN^+, C_2N^+, HC_3N, HC_3N^+, NO, NO^+, Met, Met^+, G, G^+, G^-

Table 2. Overview of reactions added to the gas phase reaction scheme of de Jong et al. (1980) and Boland (1982). Reactions involving metals in the gas phase are described by Prasad and Huntress (1980), Mitchell et al. (1978), and Graedel et al. (1980). For grains the reactions involving charge, accretion, surface reaction, monolayer formation and explosive release triggered by grain-grain collisions are described in the text. The symbols G, X, XG, and XGI represent respectively grains, species in the gas phase, on a grain surface or inside the accretion mantle, X, X^+, and X^- symbolize neutral, positive and negative gas phase species

Gas phase reactions involving metals		
i) Ionization		
1	$Met + h\nu \rightarrow Met^+ + e^-$	
ii) Electron recombination		
2	$Met^+ + e^- \rightarrow Met$	
iii) Charge exchange with ions		
3	$Met + X^+ \rightarrow Met^+ + X$	
Reactions involving grains		
i) Grain charge		
4	$e^- + G \rightarrow G^-$	Accretion rate
5	$e^- + G^+ \rightarrow G$	Enhanced accretion rate
6	$X^+ + G \rightarrow X + G^+$	Accretion rate
7	$X^+ + G^- \rightarrow X + G$	Enhanced accretion rate
ii) Accretion		
8	$X + G \rightarrow XG + G$	Accretion rate
iii) Surface reaction		
9	$XG + YG \rightarrow XYG$	Surface rate
iv) monolayer formation		
10	$XG \rightarrow XGI$	Monolayer accretion rate
v) Ejection by grain-grain collision		
11	$XG + G \rightarrow X + G$	Grain-grain collision rate

further reactions are no longer possible. The net concentration of unsaturated species e.g. radicals, in the mantle can then be calculated. The effect of UV photolysis is not included in this section: any solid phase photochemical reaction scheme would be far too uncertain and complex to be taken into account by the scheme we present here. However, the release of molecules from mantles of grains which contain free radicals, produced either by accretion or photolysis will be included in the discussion.

2.2.1. Gas-grain interactions

2.2.1.1. Sticking coefficient. When an atom, radical or molecule strikes the solid surface of a grain, it should quickly thermalize ($\tau < 10^{-11}$ s) at the surface and stick to it. The sticking rate for gas phase particles is simply given by

$$R = S\sigma\bar{v} \quad \mathrm{cm^3\,s^{-1}}, \tag{1}$$

where S is the sticking coefficient which can take any value from 0 to 1, σ the grain cross section, and $\bar{v}$ the mean thermal velocity of the gas particle, $(8\,kT/\pi m)^{1/2}$.

There is little doubt that the sticking coefficient is close to unity for all molecules considered (except for H_2) onto 0.1 μm radius grains at 10 K. There are essentially two reasons for this. Firstly, the kinetic energy of a gaseous particle between 10–100 K is much less than its adsorption energy on the substrate ($kT \ll E_b$ e.g. for NH_3, kT at 10 K is 0.027 eV while the binding energy E_b of NH_3 to the surface of a molecular ice is well in excess of 0.1 eV for pure physisorbtion). Secondly, even if the particle should possess more kinetic energy, the thermalization time is expected to be so short that the particle should lose most of its energy to the grain within a few periods of vibration ($< 10^{-11}$ s) and remain trapped on the surface (McCarrol and Erlich, 1963).

Caution should be taken in directly using laboratory measured sticking coefficients of atoms or molecules on any substrate because re-evaporation times, even at 10 K, can be very fast if the binding energy to a particular surface is low. For molecules where the binding energies are known to be greater than about 900 K [e.g. 950 K for CO on CO, Shinoda (1969), and 4000 K for H_2O on H_2O, Hale et al. (1981)], the sticking coefficient as required by Eq. (1) is unity. For atoms and radicals, binding energies are much more difficult to determine experimentally and as with molecules, must depend on the nature of the surface. According to Hollenbach and Salpeter (1971) and more recently to Burke and Hollenbach (1983), calculated accomodation coefficients and energy transfer from an incident particle to a grain surface lead to high values of the sticking coefficient even for hydrogen atoms on H_2O ice, silicate, and graphite between 10 and 100 K.

In view of the above, it is somewhat surprising that, while it is generally accepted that the H_2 molecule is exclusively made on grain surfaces, necessarily implying a high sticking coefficient for H atoms, the possible accretion of heavier atoms, radicals and molecules which simultaneously strike the grains is not considered in most interstellar chemistry models.

2.2.1.2. Grain charge. The interaction between charged species (electron and ions) and grains is considered in this section. In a dense cloud were $A_v \gtrsim 2$, photoelectric effects producing positively charged grains are negligible due to the high ionization potentials of presumably abundant molecules on interstellar grains such as H_2O, CH_4, and NH_3 for which the ionization potentials are 12.6, 13.0, and 10.2 eV respectively (Watson, 1974). In this situation, most grains are expected to be charged negatively because of the larger velocity of electrons compared to positive ions. Although the sticking coefficient of electrons on a grain surface is not very well known, theoretical calculations by Umebayashi and Nakano (1980), based on the energy exchange between the incident electron and the grain lattice via phonon excitation, show that it should be close to unity. Experiments to measure the sticking coefficients of low energy electrons on neutral surfaces, such as graphite, are consistent with these calculations (Lander and Morrison, 1964). Sticking coefficients of electrons and ions with charged surfaces are not known but fortunately, as shown below, play a less important role in the overall process.

Assuming a sticking coefficient of one for electrons and that they are mobile and confined to the surface, one can approximate the maximum charge a grain can accumulate at its surface. The cross section for accretion of a charged particle when the grain possesses a charge Q_d is:

$$\pi a_{Q_d}^2 = \pi a_d^2 \left(1 - \frac{2Q_p Q_d}{a_d m_p v_p^2}\right), \tag{2}$$

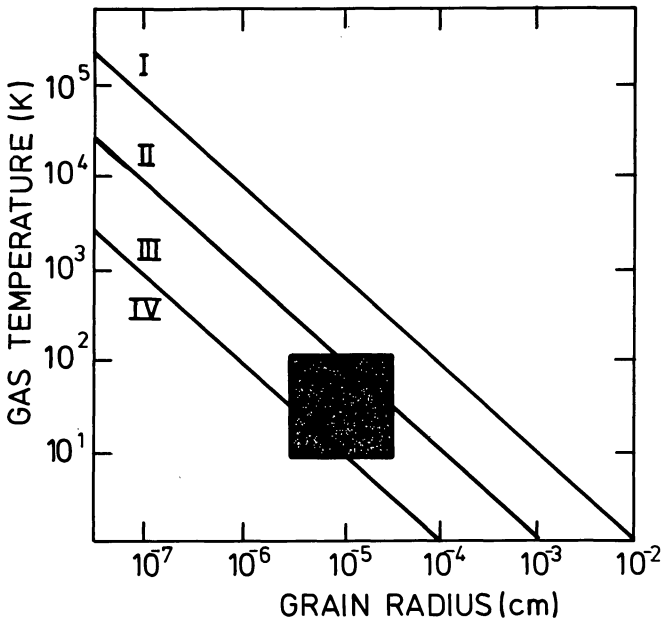

Fig. 1. Regions of grain charge as a function of gas temperature and grain radius. The charge l is calculated with Eq. (3) taking only accretion of charged species (electrons and ions) into account. No photoelectric effect is assumed. *Region I*: $Q_d > 7.6e+1e$. *Region II*: $0.76e+1e < Q_d < 7.6e+1e$. *Region III*: $0.076e+1e < Q_d < 0.76e+1e$. *Region IV*: $Q_d < 0.076e+1e$. The area in the shaded box which encompasses the range of interstellar cloud conditions treated in the model shows that region III is the most applicable. For the standard case ($a \cong 10^{-5}$ cm, $T = 50$–100 K), the maximum charge is taken as -1

where a_d and a_{Q_d} are the radii of the neutral and charged grain, Q_d the charge of the grain, $\frac{1}{2} m_p v_p^2$ represents the kinetic energy of the incident particle, and Q_p represents the charge of the gas particle (e.g. Spitzer, 1978). In cold interstellar cloud, we can assume that $Q_p = 1$. From Eq. (2), it is easy to derive the value Q_d for which accretion is impossible ($\pi a_{Q_d}^2 = 0$) and we obtain

$$l = \frac{a_d k T_g}{2e^2}, \tag{3}$$

where l represents the maximum possible charge at the surface of the grain, expressed in number of unit charge. Different domains for the values of l are outlined in Fig. 1 as a function of grain radius and gas temperature. This shows that grains in molecular clouds, where $a_d \cong 10^{-5}$ cm and $10\,\mathrm{K} \leqq T_{\mathrm{gas}} \leqq 100\,\mathrm{K}$, generally acquire a maximum charge of about $1\,e^-$. Thus, for the simplicity of the calculations, three kinds of charged grains have been considered: G^+, G, and G^- (representing positive, neutral, and negative grains) while ignoring higher grain charges (e.g. G^{2+}, G^{2-}). This approach is supported by the more complete treatment of grain charge determination carried out by Umebayashi and Nakano (1980). In calculating the actual charge distribution of the grains under similar conditions, they show that, in the absence of the photoelectric effect, grains charged higher than one can be disregarded.

The surface reactions which determine the charged grain distribution at each time step are numbers 4 through 7 in Table 2. For positive ions interacting with negatively charged grains, we follow Watson (1974) and assume that recombination of an ion on a negative grain surface neutralizes both the grain and the ion and that the neutral specie formed leaves the grain because the recombination energy which resides largely with the ion is much greater than the binding energy and cannot be accomodated by the grain. These neutralization reactions greatly simplify the treatment of surface reactions since they reduce the number of different species which can accrete on grains.

2.2.2. Surface reactions

Once a reactive gas phase specie has landed on the grain, its binding energy to the surface will determine whether it will be immobile, diffuse on the surface or evaporate. If it remains on the surface it will eventually either react with another adsorbed reactant, provided that the activation energy for a particular reaction is low, or become integrated in the mantle where it cannot react any further. The former route leads to the build-up of new molecules, the latter to trapped radicals. The net concentration of trapped radicals can then be calculated.

2.2.2.1. Binding energy and surface mobility. Due to the over-abundance of hydrogen (atomic and molecular) one expects that the chemically reactive sites on a grain surface will be quickly hydrogenated and that incoming particles on top of this layer will be bound by weak forces, primarily involving only physisorption mechanisms (Watson and Salpeter, 1972). Because of the low gas phase temperatures expected in dense clouds ($10 < T_g < 100$ K) as well as for the grains ($10 < T_d < 20$ K), we do not consider the process of catalytic chemisorption in which a bond of the incoming molecule or radical is broken, with the fragments now "poised" for further reaction with other surface species while attached to the surface with strong chemical forces. The activation energies for such processes are high (a few eV, Redhead et al., 1968), precluding their occurrence at the typically low interstellar temperatures. Thus, the role of the grains in molecular clouds cannot be called catalytic in the strict sense of the word and the surface can be considered as not particularly reactive.

For physisorption, binding energies for pure substances are well known because they can be deduced from the known vapour pressure of these substances. For mixtures and radicals, the situation is less clear and the value of the binding energy will depend on the surface considered. The binding energy for H_2 on frozen H_2O and CO has been measured to be 860 K and 350 K (Lee, 1972), values of 750 K and 280 K for H on H_2O and CO can be expected form the ratio of the polarizabilities of H to H_2 (Watson, 1974). Binding energies in excess of 800 K are expected for the reactive atoms C, N, and O; values greater than 1000 to 2000 K are taken for small unsaturated molecules (Watson and Salpeter, 1972).

2.2.2.2. Surface mobility: rates and timescales. We define here the basic rates for re-evaporation, surface migration and accretion from the gas phase in order to describe a simplified solid phase scheme which takes into account the main features of the low temperature chemistry possible on the surface of a grain in the absence of an external source of energy.

As already defined, the accretion rate from the gas onto the grain is given by

$$R = S \sigma \bar{v} \quad \mathrm{cm^3\,s^{-1}}. \tag{1}$$

If either of the reactive species is mobile on the surface of the grain, the cross section of a surface reaction for an accreting specie is given by σ_d, the total surface of the grain. If, on the other hand, neither of the two reactants is mobile, the cross section drops formally to the value σ_m, the cross section of the molecule itself and

because σ_m is many orders of magnitude smaller than σ_d, different processes can dominate. In this case the reaction rate can become slower than the rates of evaporation, coverage by saturated molecules and reactions with H atoms thus quenching the reaction between immobile species. Site residence times are computed with the following equations:

$$\tau_{ev} = \nu_0^{-1} \exp(E_b/kT_d) \quad \text{s} \quad \text{(re-evaporation time)}, \tag{4}$$

where E_b represents the binding energy of the particle, T_d the temperature of the dust grain, ν_0 the frequency with which the particle oscillates in its site, and k, the Boltzman constant.

For diffusion, two processes must be considered: quantum mechanical tunnelling and thermal hopping. These timescales can be computed from:

$$\tau_t = \nu_0^{-1} \exp\left\{\frac{2a}{\hbar}(2mE_b^{1/2})\right\} \quad \text{s} \quad \text{(tunneling time)}, \tag{5}$$

$$\tau_D = \nu_0^{-1} \exp(E_D/kT_d) \quad \text{s} \quad \text{(thermal diffusion time)}, \tag{6}$$

where a represents the lattice spacing ($\approx 10^{-8}$ cm), $\hbar = h/2\pi$, h represents the Planck constant, m the mass of the diffusing specie and E its binding energy. In the case of thermal diffusion of species bound by physisorption, the barrier against diffusion E_D can be approximated by the value $E_b/2$ as shown in experiments involving second layer diffusion on top of a monolayer of adsorbed species (Folman and Klein, 1968).

We shall consider quantum tunneling only for the hydrogen atom. Heavier abundant atoms or radicals (atomic mass $\geqq 12$) cannot tunnel because of their mass (Salpeter, 1971). *The high mobility* ($\tau_t \simeq 10^{-11}$ s) *and abundance of the H atom will make it by far the preponderant reactant with any unsaturated molecule on the surface*, for all values of A_v less than about 5.

The two next important timescales to consider are the timescale for scanning the entire surface of the grain (τ_{sca}) and the average timescale for the accretion of a monolayer of saturated molecules from the gas (τ_{ml}) which will prevent further reaction by burying the reactive specie in the mantle where its binding energy will not allow further diffusion. These timescales are given by:

$$\tau_{sca} \simeq N^2 \tau_D \quad \text{s}, \tag{7}$$

where N represents the number of surface sites available (for a 0.1 μm radius grain, $N \cong 10^6$) and τ_D the time needed for one jump [Eq. (5)] and

$$\tau_{ml} \simeq N(n_{O,C,N}\sigma_d \bar{v})^{-1} \quad \text{s} \tag{8}$$

with $N_{O,C,N}$ collectively representing the number density of heavy atoms by cosmic abundance in the gas phase, N the number of surface sites, σ_d the grain cross section for accretion and $\bar{v}$ the mean kinetic velocity of the gas phase particles. For tunneling, the timescale for scanning the entire grain is somewhat shorter because the tunneling process is not completely random (Hollenbach and Salpeter, 1970, 1971; McCarroll and McKee, 1971). In this particular case, the scan time is given by

$$\tau_{sca} \sim N^{\alpha}\tau_t \quad \text{where} \quad 1 \leqq \alpha \leqq 2. \tag{9}$$

For an hydrogen atom, $\tau_{sca} \sim 10^{-5}$ s ($\alpha = 1$, Hollenbach and Salpeter, 1971) implying that the hydrogen atoms are completely delocalized at the surface of the grains. This scanning time is very short compared to the other timescales described above.

These different timescales are plotted as a function of binding energy for different grain temperatures in Fig. 2. From this figure, it is clear that, for species with a binding energy of 800 K, on 10–12 K grains, $\tau_{ev} > \tau_{sca} > \tau_{ml}$. Thus, binding energy determines the ability of the reactive species of interest to make new molecules. Thermal re-evaporation is negligible at 10–12 K. Scanning of the surface by heavy atoms is indeed a slow process compared to the scanning by hydrogen atoms so that radical-hydrogen reactions are favored as long as H atoms are at least as abundant as the heavier atoms. Finally, once atomic hydrogen has been converted to molecular hydrogen, reactions between the heavier atoms and radicals take place. However, because the time to acquire a monolayer is short compared to the scan time one can expect a certain fraction of radicals to be trapped within the mantle.

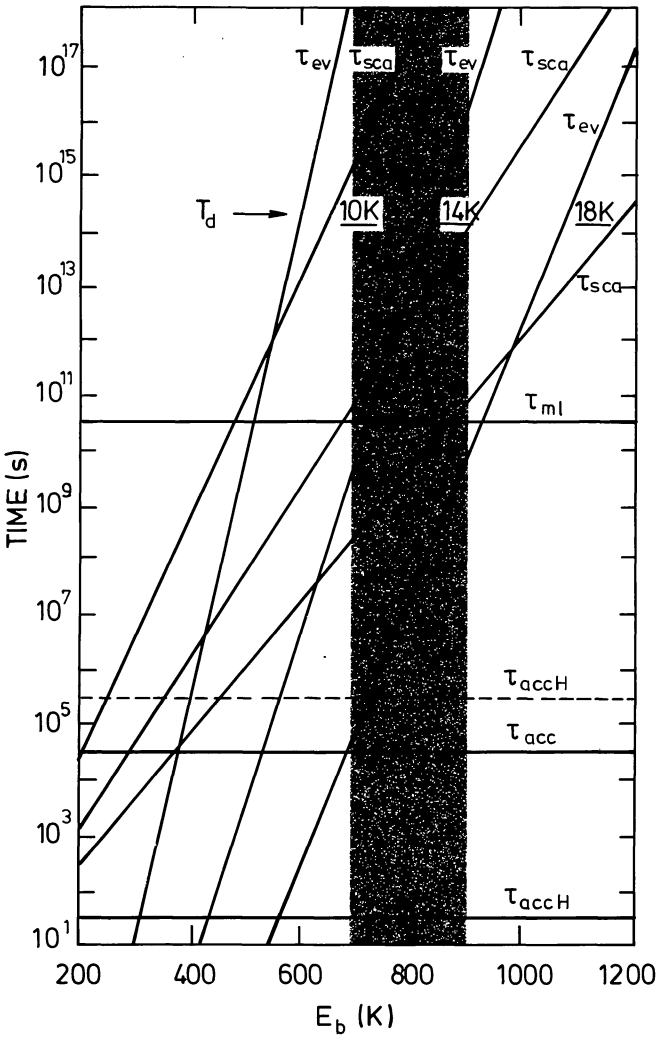

Fig. 2. Monolayer formation, accretion, evaporation and surface scanning timescales for 0.1 μm radius grains as a function of binding energy for different grain temperatures. τ_{ev} and τ_{sca} represent, respectively, the evaporation and grain surface scanning time for the atoms O, C, N. τ_{acc} and τ_{ml} indicate accretion and monolayer formation times. Accretion times for hydrogen are given by τ_{accH} with the solid line representing the case when H is mainly atomic and the broken line when it is molecular. The binding energy for heavier atoms and molecules on ice mantles lie in the 700–900 K range as indicated by the shaded area

2.2.2.3. Surface reactions: rates and activation energies. From Eqs. (5) and (6) it is possible to derive a surface reaction rate with notation completely analogous to that used in describing gas phase

reactions. This rate is expressed as

$$R = a^2/\tau_D \quad \mathrm{cm^2\,s^{-1}}, \tag{10}$$

where a represents the lattice spacing and τ_D the time required for one jump, either from thermal hopping or tunneling. For practical purposes this rate in $\mathrm{cm^2\,s^{-1}}$ is converted to a spatial rate in $\mathrm{cm^3\,s^{-1}}$ by scaling the available surface of one grain to one $\mathrm{cm^3}$ in the gas phase as follows

$$R = \frac{a^2}{\tau_D}\,\frac{1}{4\pi a_d^2 n_d} \quad \mathrm{cm^3\,s^{-1}}, \tag{11}$$

where a_d is the radius of the grain and n_d the number density of grains. For consistency, the concentration of surface species is given in the same units ($\mathrm{cm^{-3}}$) as gas phase molecules.

Because of the low temperature of the grains, we shall consider only reactions between atoms and radicals where the activation energy is known to be zero. Radical reactions with a molecule where the reaction involves the breaking of a chemical bond are expected to have significant activation energies and are not taken into account (Tielens and Hagen, 1982). Moreover, at 10 K, even reactions with an activation barrier as low as 1000 K will be of statistically negligible importance. (The list of reactions used in the model is given in Table 4. The radicals HCO and OH become abundant enough at long times of evolution to interact because they are made efficiently on grains via the activationless reactions

$$\mathrm{H + O \rightarrow OH}$$
$$\mathrm{H + CO \rightarrow HCO}.$$

To take this into account, a few radical-radical recombination reactions have been included involving these very abundant radicals (reactions 16, 17, and 18; Table 4). It is assumed that they proceed with zero activation energy.

Useful information about the diffusivity and the solid state reaction rates of astrophysically relevant species can now be obtained from laboratory experiments using low temperature solid matrices (see for example Hallam, 1973). For example, the reaction $\mathrm{H + CO \rightarrow HCO}$ (I) has been included but not $\mathrm{H + HCO \rightarrow H_2CO}$ (II) since (I) has been shown to have a negligible activation energy and proceeds between 10 and 15 K in a solid matrix, while reaction (II), which apparently possesses a non-negligible activation energy, only slowly occurs at temperatures above 25–30 K. In these experiments, it was found that HCO preferentially reacts with another formyl radical rather than an H atom, producing the molecule glyoxal, $\mathrm{C_2H_2O_2}$ (Van IJzendoorn et al., 1983, 1985). In order to maintain consistency between gaseous and solid state species, glyoxal, a stable molecule is treated only as an intermediate which ultimately yields the thermodynamically more stable species $\mathrm{H_2}$ and 2 CO, rather than CO and $\mathrm{H_2CO}$.

The role of another, potentially important but controversial reaction, $\mathrm{CO + O \rightarrow CO_2}$ (III) has also been studied with this type of experiment. While an activation energy of 1000 K for reaction (III) has been deduced by Fournier et al. (1979) and Mohammed et al. (1980), Tielens and Hagen (1982) deduced a negligible activation energy from laboratory experiments involving the UV photolysis of CO and $\mathrm{O_2}$ containing matrices at low temperatures. Warming up from 10 to 15 K led to an increase in the $\mathrm{CO_2}$ infrared band strength, consistent with the occurrence of reaction III, implying that the reaction proceeds with a negligible activation energy. However, we have found that warm-up of photolyzed matrices ($\mathrm{Ar : CO : H_2O}$; 300 : 1 : 1) while effecting the band shape between 10 and 20 K, did not enhance the integrated $\mathrm{CO_2}$ absorption peak significantly although the well-known $\mathrm{O_2}$ chemiluminescence, due to the reaction $\mathrm{O + O \rightarrow O_2}$ (Smardzewski, 1978) was observed along with $\mathrm{O_3}$ formation showing that oxygen atoms were present and diffusing sufficiently to encounter reactive partners (Grim and d'Hendecourt, 1985). We conclude therefore that reaction III possesses some activation energy and should be disregarded. However, due to the controversial nature of this particular reaction, how it affects the results will be briefly discussed.

2.2.3. Molecule ejection

The problem of molecule release from interstellar grains has been discussed by many authors and will only be briefly reviewed here. Useful references can be found in Watson and Salpeter (1972), Allen and Robinson (1975), and Tielens and Hagen (1982). Molecules can be released from grains by various processes such as: direct ejection upon formation on the surface of the grain, thermal evaporation due to the heating of the entire grain following an exothermic molecule formation reaction, thermal evaporation, and finally enhanced evaporation mechanisms such as photodesorption, cosmic-ray desorption and chemical instability due to the trapping of reactive species frozen in the mantle (Greenberg, 1979).

Direct ejection from the surface following recombination of two atoms is believed to be efficient for $\mathrm{H_2}$ (Hollenbach and Salpeter, 1970) and, as the binding energy of $\mathrm{H_2}$ on any substrate tends to become small at one monolayer coverage (Lee, 1972), thermal evaporation of the $\mathrm{H_2}$ molecule will occur rapidly. For heavier molecules, the situation is less clear. If the coupling of the adsorbed molecule to the surface is strong, the energy transfer to the surface should be efficient and ejection will not occur. Non-saturated molecules (OH, CH) as well as molecules, with high binding energies due to hydrogen bonding ($\mathrm{H_2O}$, $\mathrm{NH_3}$) will probably remain on the surface whereas symmetrical, saturated molecules such as $\mathrm{CH_4}$ are likely to leave the grain upon formation. Unfortunately, the efficiency of the release is very poorly known and is believed to be low (Watson and Salpeter, 1972). We have chosen, in general, to adopt the hypothesis of non-ejection upon formation.

A saturated molecule directly accreted on the grain will not be subject to any of these release mechanisms and another desorption mechanism must be available to counterbalance accretion in order to prevent complete depletion of all gas phase species onto the larger grains. Thermal evaporation due to heating of the entire grain following a surface recombination reaction has been investigated by Allen and Robinson (1975). However, this process will not lead to ejection for grains larger than about 50 Å in radius and does not preclude accretion on larger grains. As described in Sect. 2.2.1.2.), thermal evaporation does not play a role as long as grain temperatures remain under 20 K for species with binding energies in excess of 800 K, the two conditions which prevail in the regions of molecular clouds under consideration. Although photodesorption has been thought to be an efficient mechanism, experimental results as well as theoretical studies raise doubts about the efficiency of the process. Yields between 10^{-6}–10^{-7} for molecules such as $\mathrm{H_2O}$, $\mathrm{CH_4}$, and $\mathrm{NH_3}$ have been experimentally measured by L. Greenberg (1973). Higher yields (10^{-2} to 10^{-4}) are required if this process is to compete with accretion. A value of 10^{-6} was used in these calculations, consistent with the values reported by L. Greenberg (1973), and used by Barlow (1978), Draine and Salpeter (1979), and Tielens and Hagen (1982). These yields are extrapolations from the lower yields measured in the regions of the spectrum where the molecules studied do not absorb efficiently (2000–2500 Å). Moreover, as reported by L. Greenberg

(1973), the yield for photodesorption goes down dramatically when one passes from first layer to second layer desorption. More recently, Bourdon et al. (1982) derived substantially smaller yields (10^{-10}) for strongly physisorbed molecules and give a cross section for photodesorption of 10^{-24} cm^2, 10^4 times smaller than the values derived by L. Greenberg (1973) and conclude that photodesorption is an inefficient mechanism for the release of adsorbed molecules on grains in dense clouds. Obviously, photodesorption is not an efficient process and requires a higher ultraviolet flux than is available in molecular clouds with $A_v > 2$. Moreover, yields lower than 10^{-7} are expected for second layer desorption so that, even mantles accumulated within a shielded region of a cloud will be difficult to photodesorb at the outside of the cloud if transported by wide scale turbulence (Boland and de Jong, 1982). Recent studies by Nishi et al. (1984) are consistent with this conclusion as they show measurable photoejection from realistic ices only upon, intense, two photon excitation or from samples with radiatively damaged surface.

Cosmic ray interactions with grains can lead to some evaporation of molecules either from the heating of the entire grain or from heating of a hot spot at the surface of the grain but the maximum rate is too low to be an efficient desorption mechanism in molecular clouds and this process has not been taken into account in our model. However, quite recently, Leger et al. (1985) argue that heavier cosmic rays (iron nuclei) than those previously considered are important for mantle desorption.

Evaporation of the grain mantle by the energy released in radical recombination and chain reactions, leading ultimately to the explosion of the mantle, has been postulated by Greenberg and Yencha (1973) as a solution to the problem of replenishing the gas phase. This process has been demonstrated in the laboratory. The experiments, as well as a short description of the astrophysical implications are described by d'Hendecourt et al. (1982). Binding energies for molecules physisorbed on grains lie in the range 1000 to 3000 K. Typical chemical bond energies are of the order of 5 eV (5.8 10^4 K) so that the radical concentration required for evaporation of the mantle is about 1 to 3% assuming an average number of bonds formed per reaction to be about 1.7. At low temperatures, certain radicals (e.g. HCO) can be isolated in sufficient concentration to provide the energy needed to drive such an explosive evaporation event. However a triggering mechanism is required to raise the temperature of the grain to the point where diffusion of the reactants leading to a chain reaction and explosion becomes possible. The onset of fast diffusion processes occurs at about 27 K in amorphous ices; to reach this in the interstellar medium, a 17 K raise in temperature is required. A more detailed discussion of the explosion mechanism can be found elsewhere (d'Hendecourt et al., 1982; d'Hendecourt, 1984). In the calculations described here, the explosive release of molecules is triggered by grain-grain collisions. Assuming that 0.1 μm radius grains are involved, implies that a collision velocity of 40 m s^{-1} is needed to raise the temperature of the grain by the required amount. In this model, all grains are assumed to be moving at this velocity and to undergo subthermal molecule ejection upon each collision. Of course, other processes such as fragmentation or coagulation might be possible but at the radical concentration calculated here, we assume that the explosive release of molecules is the dominant mechanism as evidenced by laboratory experiments. The equation corresponding to the release of molecules in the computer model is number 11 in Table 2.

Although this process occurs in the laboratory at low irradiation levels, in a quiescent interstellar cloud where the visual extinction (A_v) becomes larger than 5, and no internal UV sources are present, photolysis of a completely saturated mantle containing no radicals initially should not produce enough stored energy to allow chemical explosions to take place (d'Hendecourt et al., 1982). In the calculated mantle however, the net concentration of stored radicals results from direct accretion and incomplete surface reaction. A concentration in excess of 1% is obtained even for high values of $A_v (A_v = 8)$ so that this explosion process can still take place although its efficiency might be reduced. If there is a low level residual UV flux inside a cloud, this reduced efficiency could be enhanced. A flux of (10^{-4}–10^{-5} of the general interstellar radiation field) has been postulated to arise from shocks inside clouds (Silk and Norman, 1980) and from interactions of cosmic rays with H_2 molecules (Prasad and Tarafdar, 1983).

2.2.4. Summary of solid state processes:

In order to compare these different processes and to assess their respective importance in different regions of the interstellar medium, the values of these desorption rates were computed as a function of density, visual extinction and gas temperature. Although the interplay between these three quantities is certainly not trivial, it is reasonable to assume that a less dense medium will be subject to more ultraviolet starlight from the diffuse medium than the higher density regions. Simultaneously, the temperature of the more diffuse medium has been taken slightly higher than that of the dense medium (Sitzer, 1978). The different rates used for each process have been computed from the following equations:

Accretion rate: $$R_{ac} = n_i \sigma_d \bar{v}_i \quad \text{s}^{-1}, \tag{12}$$

UV grain collision rate: $$R_{UV} = G_0 \exp(-2A_v)\sigma_d \quad \text{s}^{-1}, \tag{13}$$

Photodesorption rate: $$R_{pd} = Y R_{UV} \quad \text{s}^{-1}, \tag{14}$$

Explosion rate: $$R_{exp} = 2 n_d v_d \sigma_d N_m \quad \text{s}^{-1}, \tag{15}$$

where n_i and $\bar{v}_i$ represent the density and kinetic velocity of the gas phase heavy particles (O, C, N, ...); σ_d, the grain cross section; G_0, the mean interstellar UV field (Habing, 1968); $\exp(-2A_v)$, the attenuation of the UV field inside the cloud; Y, the photodesorption yield; n_d, the grain number density; v_d, the grain velocity for grain-grain collisions; and N_m, the number of molecules per grain mantle. The following parameters have also been used:

$$n_{OCN} = 10^{-3} n_H$$
$$n_d = 10^{-12} n_H$$
$$a_d = 0.1\ \mu\text{m}$$

Theses rates are plotted in Fig. 3 as a function of selected sets of values of density, visual extinction and gas temperature which should be representative of different regions of the interstellar medium. The evaporation rate from cosmic-ray collisions as deduced by Watson and Salpeter (1972) is also given. However, as already mentionned, Léger et al. (1985) have deduced a higher evaporation rate from the interaction of heavy nuclei cosmic-ray (iron nuclei). In their model, they calculate the possibility for these heavy nuclei cosmic rays to generate the chemical explosion because the energy deposition of these nuclei in the mantle is sufficient to raise its temperature to the critical point where the explosion can take place. This process will allow and efficient desorption mechanism to exist comparable in magnitude to the one given by the low velocity grain-grain collisions. A yield of 10^{-4} has been used for photodesorption, two orders of magnitude larger than the one measured by L. Greenberg (1973) and six orders larger than that measured by Bourdon et al. (1982). Greenberg's explosion mechanism is a much more efficient process provided the

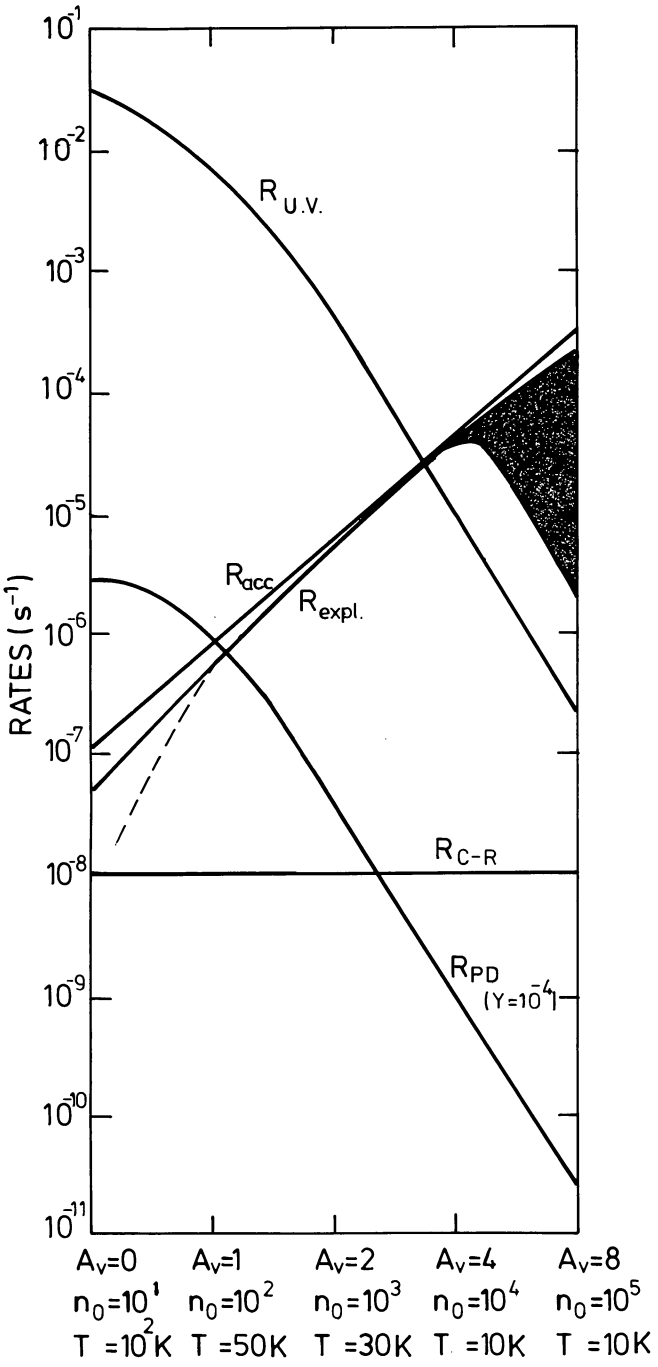

Fig. 3. Accretion and desorption rates used versus cloud parameters. For desorption, explosion (R_{expl}) photodesorption (R_{PD}) and cosmic-ray interaction (R_{C-R}) rates are given. Accretion and UV photon-grain collision rates are indicated by R_{acc} and R_{UV}. The hatched area corresponds to the uncertainty introduced in the rate of the explosion process when the UV field is reduced. For low extinction values ($A_v < 1$), photodesorption dominates and explosive desorption is no longer applicable (dotted line). For $1 < A_v < 5$, $R_{expl} \simeq R_{acc}$. For $A_v > 5$, the maximum decrease in the explosive desorption rate (lower boundary of cross-hatched area) is calculated assuming that the efficiency of the process depends linearly on the actual number of UV photons hitting the grain and requiring that the ratio of incident photons to the number of mantle molecules cannot be less than 0.1

total extinction does not attain very high values ($A_v > 5$). However for higher values of extinction, the minimum concentration of radicals required can be achieved on a longer time scale, permitting this process to occur with reduced efficiency. The hatched zone in Fig. 3 indicates the possible uncertainty.

3. Results

Equilibrium values for the different species depend on certain initial parameters such as the elemental abundances, the degree of ionization by cosmic-rays, the UV radiation field and to a lesser extent the density and the temperature of the gas. Thus, in a time dependent calculation it would be tedious, if not impossible, owing to the number and complexity of the results, to vary and discuss all the different parameters in detail. Moreover, a great deal of effort concerning the gas phase chemistry has already been made to assess the importance of these various parameters (see, for example, Graedel et al., 1982 and references therein); rather it is the purpose of this paper to investigate the effects solid state reactions will have on the gas phase as well as on the grain composition. These effects will be discussed within a restricted set of initial conditions and physical parameters. All calculations are made at a given density and visual extinction. Once these parameters are fixed, the relevant solid state reactions are discussed. Gas phase parameters such as optical depth and density can then be changed in order to determine their influence on the results. Initial conditions are not changed: starting abundances have been chosen which are deduced from observations of the more diffuse medium. Initial abundances for all molecules, *including* H_2, are set to zero. Implicit in this approach is the assumption that the basic material for the gas phase chemistry which takes place in the denser medium comes from the diffuse medium. In order to investigate the effect of initial elemental abundances on the mantle composition, four different sets of elemental abundances will be used and are discussed later as separate cases. We assume that the elements missing from the gas make up the grain cores which act as sites for subsequent reactions and mantle growth. These bound elements are thus permanently removed from the gas phase and not taken into account in this calculation. Consistent with diffuse cloud observation, we assume that initially, carbon and the metals are ionized and that the electron abundance is equal to the value of the sum of the ionized species. These different initial conditions are summarized in Table 3. Gas and solid phase abundances are obtained as a function of time between 10^4 and 10^8 years, assuming that initially all the gas is in atomic form, including hydrogen, with the conversion of H to H_2 and the accretion of heavy species

Table 3. Elemental abundances and cloud parameters used for the standard case. The abundances, all given with respect to H, have been measured for ξ Oph, and are taken from Morton (1974), de Boer (1981), and Lugger et al. (1978). *Standard model*: $A_v = 4$; $n_0 = 2\ 10^4\ \mathrm{cm}^{-3}$ ($n_0 = n_H + 2n_{H_2}$)

Elemental abundances		Cloud conditions	
He	10^{-1}	n_d	$= 10^{-12} n_H$
O	$5.01\ 10^{-4}$		
C	$1.58\ 10^{-4}$	a_d	$= 10^{-5}$ cm
N	$6.31\ 10^{-5}$	T_{gas}	$= T_{dust} = 10$ K

followed by surface reactions taking place simultaneously (Table 4). For the standard case (hereafter referred to as the standard model), the elements available in the gas phase are those determined from depletion measurements in the ξ Oph cloud as given in Tables 3 and 9. However, because the depletion measurements vary from cloud to cloud and because different elemental composition results in quite different mantle composition (Tielens and Hagen, 1982), this aspect is discussed separately in Sect. 3.3.2 below with particular emphasis on the importance of the O/C ratio for the chemistry of the mantles. The abundances of the metals are the ones actually observed in the diffuse medium and correspond to the high metal abundances described in Graedel et al. (1982). We assume that the initial carbon and metals are ionized, all the other elements being neutral. Naturally, the electron abundance is taken as the sum of the ion abundances to ensure the charge neutrality of the whole system. The standard model also assumes a density $n_0 = 2\ 10^4\ \mathrm{cm}^{-3}$ ($n_0 = n_H + 2n_{H_2}$) and a visual extinction $A_v = 4$. How the composition varies as a function of these parameters will also be discussed.

3.1. *Simple accretion model*

Although the problems raised by considering the effects of accretion on a gas phase, time dependent chemistry scheme was considered by Iglesias (1977), we present this example here again as an important justification of our study by demonstrating the straightforward effect accretion has on gas phase molecule abundances. The main result is shown in Fig. 4 for several species. In this calculation, except for helium and hydrogen, atoms, radicals or molecules do not return to the gas phase once they have struck a grain. The hydrogen molecule is made on the grains and returned to the gas phase. Positive ions, including metal ions, are returned to the gas phase as neutrals upon collision with the grains. This process tends to slow down somewhat the accretion rate as illustrated by the delayed drop in the metal ion abundance. Molecular abundances, which always remain low, are inconsistent with observations in spite of the fact that the CO molecule is quickly formed in the gas phase. Accretion dominates within 10^6 years, slower than in Iglesias' model because the average surface area of the grains used in our calculation ($a_d = 0.1\ \mu$m) is smaller ($a_{\mathrm{Iglesias}} \simeq 0.25\ \mu$m). An average grain radius of 0.1 μm and a gas-to-dust ratio given by $n_d = 10^{-12} n_H$, provides a mean surface area of grain per hydrogen atom of $5\ 10^{-22}\ \mathrm{cm}^{-2}$, compatible with the interpretation of observations as described by Greenberg (1978). As already pointed out, H_2 formation proceeds at rates similar to the accretion rates of heavy species. Thus, in clouds where H_2 is dominant, one can be confident that the molecules observed in the

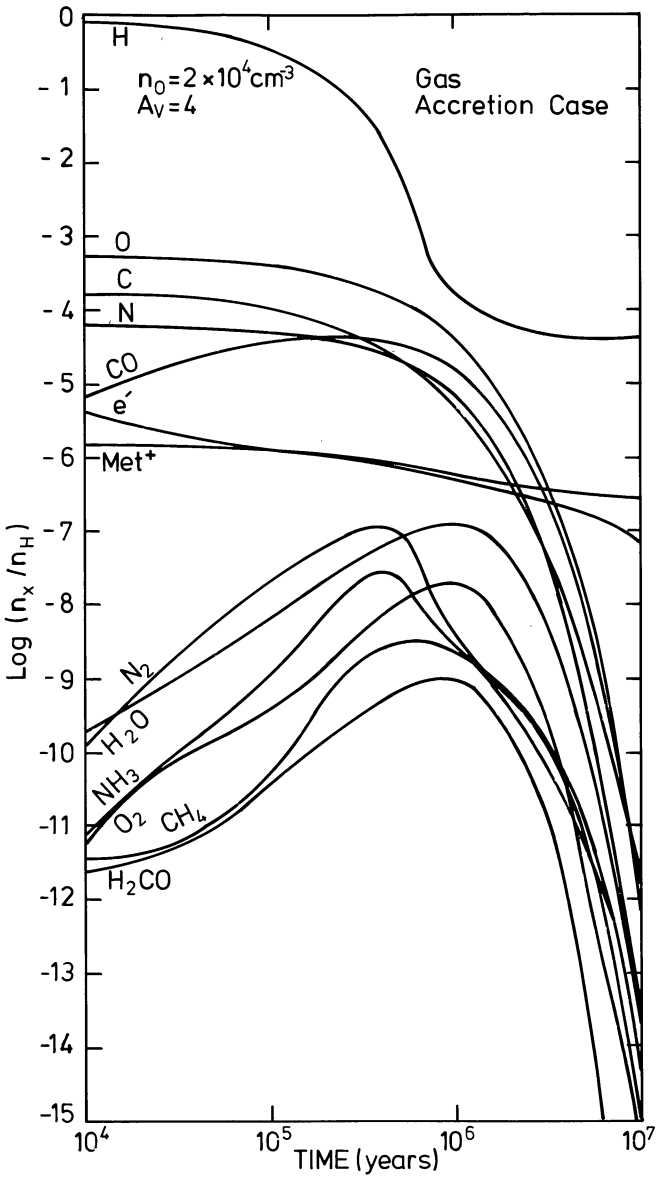

Fig. 4. Time evolution of gas phase abundances for the accretion model. Not all species are shown

Table 4. List of grain surface reactions involving heavy atoms included in the grogram

	Reactions			Ref.
1	$H + CO$	$\rightarrow$	HCO	a
2	$H + C$	$\rightarrow$	CH	b
3	$H + CH$	$\rightarrow$	CH_2	b
4	$H + CH_2$	$\rightarrow$	CH_3	b
5	$H + CH_3$	$\rightarrow$	CH_4	b
6	$H + N$	$\rightarrow$	NH	b
7	$H + NH$	$\rightarrow$	NH_2	b
8	$H + NH_2$	$\rightarrow$	NH_3	b
9	$H + O$	$\rightarrow$	OH	b
10	$H + OH$	$\rightarrow$	H_2O	b
11	$C + N$	$\rightarrow$	CN	b
12	$O + O$	$\rightarrow$	O_2	c
13	$O + N$	$\rightarrow$	NO	d
14	$O + C$	$\rightarrow$	CO	d
15	$O + CO$	$\rightarrow$	CO_2	e
16	$HCO + HCO$	$\rightarrow$	$[H_2C_2O_2] \rightarrow H_2 + 2CO$	e
17	$HCO + OH$	$\rightarrow$	$CO + H_2O$	e
18	$OH + OH$	$\rightarrow$	$H_2O + H$	e

References: a) Van IJzendoorn et al. (1983). b) Atom-atom reactions and H atom-radical reactions are assumed to proceed with negligible activation energy. c) Smardzewski (1978). d) Van de Bult et al. (1980). e) See text

Table 5. Percent compositions of main grain mantle components in the simple accretion model after complete accretion with and without surface reactions

Without surface reactions		With surface reactions	
O	63.9	H_2O	65.3
H_2O	–	CH_4	14.3
OH	1.2	CO	10.1
O_2	–	NH_3	9.3
C	6.2	CO_2	0.4
CO	18.4	O_2	0.3
N_2	0.2	N_2	0.1
NH_3			

gas phase have encountered the grains and grain surface processes should be taken into account. Finally, if one does not take surface reactions into account, the accretion of gas phase species produces a mantle whose composition, given in Table 5, reflects the fact that accretion is a fast process compared to ion-molecule gas phase reaction timescales. Moreover, without surface reactions, water is never sufficiently abundant in the mantle to produce the observed 3.1 micron ice band (e.g. Tielens and Hagen, 1982).

3.2. *Standard model*

The time evolutions of gas and solid phase species is shown in Fig. 5 for the standard case, with abundances presented in the same units in order to allow direct comparison between the two phases. For the gas phase species, the general trends inherent to ion-molecule schemes as discussed for example by Prasad and Huntress (1980) or Graedel et al. (1982) remain. In addition however, grains release an important quantity of neutral species back to the gas as either radicals or, mainly, saturated molecules (e.g. H_2, H_2O, CH_4, NH_3, CO, HCO, OH, CH, CH_2, CH_3, NH, NH_2). Moreover, efficient ion-recombination on negative grain surfaces also produces neutral gaseous species and decreases the ion and, hence, the electron abundances. As in classical gas phase models and, in particular, that of Boland (1982) from which our gas phase scheme derives, most of the available carbon is quickly locked up in CO.

The conversion of atomic to molecular hydrogen occurs within 10^6 years. This has a dramatic effect on the time evolution of the mantle composition since molecules such as H_2O, CH_4 and NH_3 are essentially made on grains at early times. For some molecules, there exists a strong disequilibrium between the gas and the solid phase at all times, with the most abundant molecules in one phase not being the most abundant ones in the other. This is particularly true for the water molecule: a high mantle concentration does not necessarily imply a high abundance in the gas phase.

In general, significant production of certain neutrals on grains tends to minimize the importance of the role of ions for the production and destruction of some gas phase molecular species. Accretion of neutrals on grains tends not only to enhance molecule production through surface reactions but also protect the adsorbed molecules from other routes of destruction in the gas phase, thus enhancing the equilibrium abundances of these molecules. Specific cases are discussed in the following sub-sections.

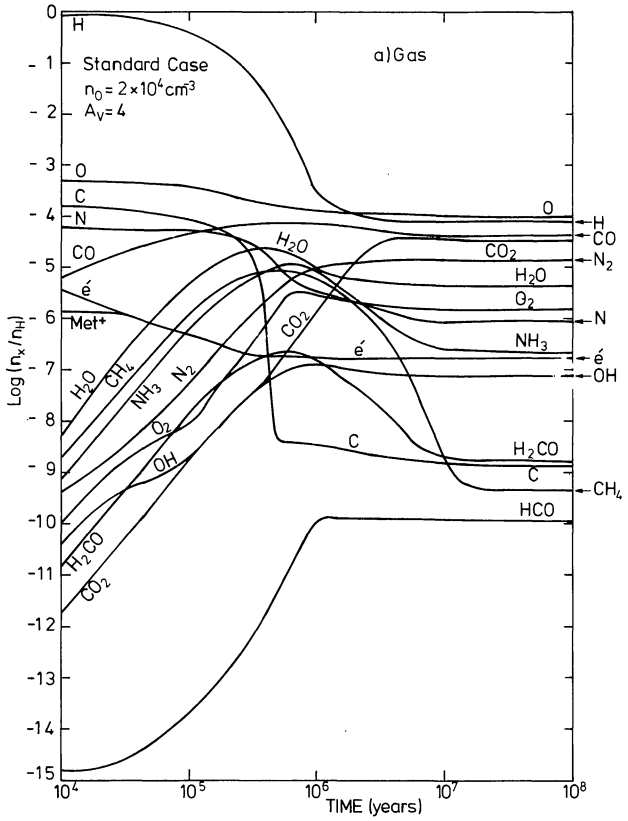

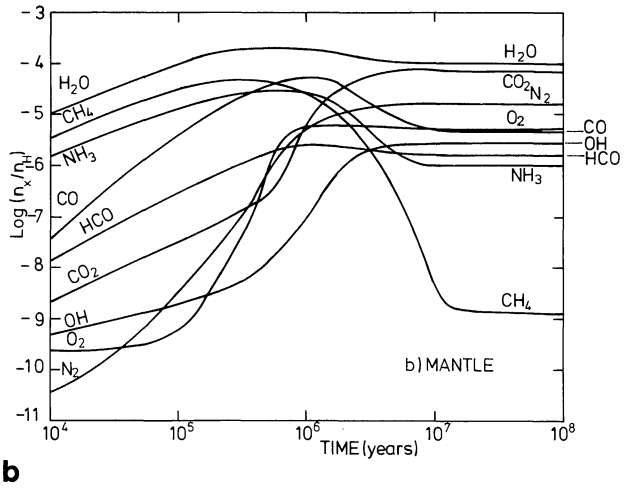

Fig. 5a and b. Time evolution of gas phase **a** and solid phase **b** abundances for the standard model ($n_0 = 2\ 10^4 cm^{-3}$, $A_v = 4$). Not all species are shown

3.2.1. Carbon bearing molecules

Neutralization of the initial carbon ions to carbon atoms is an extremely fast process which takes place within 10^4 years. Electron recombination is the most important channel but the process is enhanced by charge exchange reactions with neutral metals and by recombination on grain surfaces.

Neutralization of C^+ by H_2 is negligible at short times because H_2 is not sufficiently abundant. Neutral carbon is then converted

very rapidly to CO by neutral-neutral reactions with the aid of the following grain chemistry: neutrals such as H_2O, OH, and O_2 are released from grains, reacting with atomic carbon in the gas via the reactions

$$C + OH \rightarrow CO + H, \quad (16)$$

$$C + O_2 \rightarrow CO + O. \quad (17)$$

OH is produced mainly from grains by the process of H_2O release followed by photodissociation in the gas phase:

$$H_2O + h\nu \rightarrow H + OH. \quad (18)$$

This reaction lead to the production of O_2 via the reaction

$$O + OH \rightarrow O_2 + H. \quad (19)$$

Consequently, because CO is such a stable molecule under this condition of extinction, atomic carbon is converted to CO very quickly, with the conversion complete in less than 10^6 years, independent of the metal abundance and the degree of ionization in the cloud. Simultaneously, about half of the neutral carbon is accreted directly on grains where, in the early stages of cloud formation ($t < 10^6$ years), reactions with hydrogen atoms lead to the efficient formation of CH_4. Once atomic carbon is no longer available, with C mostly bound in CO, the production of CH_4 drops dramatically and eventually, CH_4 disappears as a major mantle constituent. In the gas phase, CH_4 is photo-dissociated mainly to form CH_2, which then reacts with atomic oxygen to form CO. Low equilibrium gas phase abundances of carbon and the stability of CO prevent carbon bearing molecules such as CH_4 from becoming very abundant even if such molecules are temporarily made efficiently on grains. It is expected that a decrease in the O/C ratio will increase the abundance of the carbon bearing molecules as discussed in the next section. The production of H_2CO in the gas at early and intermediate times is largely due to the neutral-neutral reaction

$$CH_3 + O \rightarrow H_2CO + H. \quad (20)$$

Again, as in the case of the production of CH_4, this reaction dominates at early and intermediate cloud ages. This neutral-neutral reaction, although theoretically possible on grain surfaces, has not been taken into account in spite of the fact that CH_3 and O are both present on the surface of the grains; their concentration is always low and their probability of reaction negligible since they react primarily with the abundant atomic hydrogen to make CH_4, OH and finally H_2O on the grains. In these calculations, the presence of H_2CO in the grain mantles results only from accretion of gas phase H_2CO. At later times, when radical reactions between heavy atoms take place because atomic H is less abundant, C has been consumed in CO and the surface concentration of CH_3 is too low to allow this reaction to take place, atomic O will react with CO, O and N to produce CO_2, O_2, and NO. Other radicals on the surface and in the mantle are HCO and OH. Similar to CH_4, a peak in the fractional abundance of H_2CO is reached at 10^6 years followed by a fast decline which parallels the gaseous C atom to an equilibrium value of $2\ 10^{-9}$. Formaldehyde destruction routes at equilibrium are photodestruction (for $A_v = 4$) and accretion on grains, but the amount of H_2CO in the mantle is always low in terms of percentage ($\sim 0.1\,\%$).

3.2.2. Oxygen bearing molecules

Because relatively high UV photodestruction rates are used in the standard case, OH, H_2O, and O_2 are easily photodissociated and oxygen will remain in the gas phase primarily in atomic form as shown in Fig. 5. For times shorter than 10^6 years, OH and H_2O are produced efficiently on grains either directly of indirectly. Re-accretion of H_2O produced on grains and ejected to the gas phase is a negligible process because H_2O is quickly photo-dissociated in the gas phase with the amount of H_2O in the grain, with respect to the gas phase, reflecting only the effectiveness of the grain reaction process. O_2 formation at the grain surface is slow and inefficient at short times and although it becomes more important at long times, its concentration in the mantle remains low and in the gas phase negligible, owing to its high photodestruction rate. O_2 formation in the gas phase is influenced indirectly by grain processes via the neutral-neutral reaction with OH (19) previously mentioned as responsible for a fast build-up of CO. For the standard model, because oxygen is far more abundant than carbon, CO formation does not consume more than 30 % of the available oxygen. The availability of oxygen atoms in the gas phase together with the relatively high concentration of hydrogen atoms, is a crucial parameter controlling the efficiency of H_2O formation on the grain surface at any cloud age. Figure 6 expresses the composition of the grain in mole % and shows that H_2O is indeed always dominant. The reduction in the total amount of water at longer times is tue to the fact that the H_2O production rate slows down when the H/H_2 ratio drops. The increase, in relative proportion, of molecules such as CO, CO_2, O_2, and N_2 shows that the slower reactions, involving heavier species, require more time to proceed. CO_2 and O_2 are made almost entirely on grains, N_2 is partly accreted and

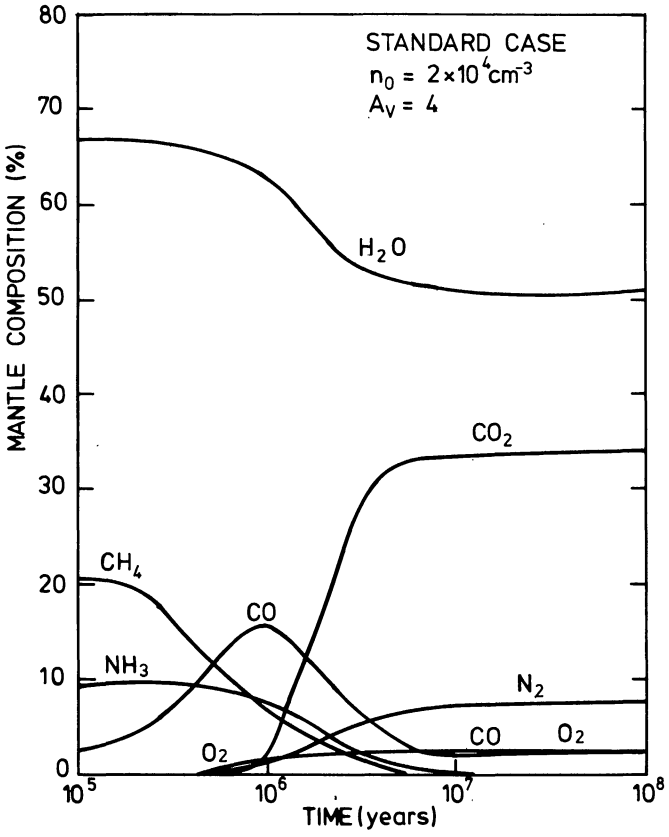

Fig. 6. Time evolution of the mantle composition for the standard model (%). Not all species are shown

partly made on grains while the CO present is largely accreted from the gas phase. The hydrogen reaction with CO

$$H + CO \rightarrow HCO \quad (21)$$

is an efficient source of stored radicals in the grain mantle.

3.2.3. Nitrogen bearing molecules

Unlike carbon, nitrogen atoms do not completely disappear from the gas phase and their residual abundance remains much higher than that for C, although they can form a very stable molecule, N_2. As shown above, carbon chemistry leads ultimately, via many reactions, to the very stable CO molecule. The nitrogen atoms, on the other hand, do not all eventually become tied up in N_2. At early stages of cloud evolution, nitrogen atoms stick onto grains forming ammonia molecules. Similar to H_2O and CH_4 formation, this is by far the main source of NH_3 in both phases. Because the amount of nitrogen atoms in the gas phase is three orders of magnitude larger than the amount of carbon, accretion and subsequent reaction of nitrogen atoms with H, efficiently produces NH_3 in the gas phase, although it is to be noted that the fractional amount of ammonia in the solid mantle is very low at equilibrium ($\sim 0.5\,\%$). Release of this ammonia to the gas phase via mantle ejection is able to maintain its equilibrium fractional abundance at the level of $2\ 10^{-7}$, a relatively high value which is more compatible with observations than values predicted by many gas phase ion-molecule schemes. This point is discussed somewhat further in Sect. 4.1.

Although CN is important, the complicated grain chemistry involving this specie has not been considered. This is justified primarily because CN can only be made at late stages on the grains by the reaction

$$C + N \rightarrow CN \quad (22)$$

or by radical reactions of the kind

$$CH_2 + N \rightarrow HCN + H \quad (23)$$

which are negligible. These and similar reactants are never abundant enough on the surface to be significant largely because nitrogen reacts almost exclusively with H to make NH_3 at the early stages and N is tied up in N_2 at later stages, C being completely absent from the mantle.

3.2.4. Metals, electrons and grain charge

As described in Sect. 2.1, metals have been treated in a manner similar to that used by Prasad and Huntress (1980) and Graedel et al. (1982). The interaction of electrons with grains, in the absence of a photo-electric effect, leads to grains with an average charge of $1\,e^-$. For gas phase electron abundances, this electron removed from the gas phase represents only a negligible fraction of the total charge (1–10 %) so that, for densities less than $10^5\,cm^{-3}$, this process alone does not significantly decrease the gas phase electron abundance. Although the initial metal abundance is consistent with observed depletion, the fractional electron abundance calculated for the standard model remains low and in reasonable agreement with observed values. Lower values are expected for higher values of extinction even if the metal content is high. There are two reasons for this: first, a small fraction of the metals permanently reside on grains, decreasing the net gas phase metal abundance and second, more importantly, metal ion recombination reactions with negatively charged grains, having a higher cross section than simple accretion, constitute an important neutralization for metal ions. Hence, during the entire lifetime of a cloud, the metals remain largely neutral (80–90 %) in the gas phase, due basically to charge exchange reactions with grains, contrary to the results calculated when taking only gas phase processes into account (e.g. Graedel et al., 1982). As a consequence, the presence of metals, in concentrations compatible with diffuse medium observations, has no serious effect upon the destruction rate of gas phase molecules: the CO molecule is abundant in our case although the metal content is high. This is directly given by a grain process. At lower densities ($n_H < 10^3\,cm^{-3}$), the role of the grains is less important because accretion and collision times, which are proportional to n_H, are longer. In low density regions, the effect of metallicity on the chemistry described by Graedel et al. (1982) becomes more important.

3.3. *Dependence on parameters*

Since the dependence of gas phase molecular abundance on various parameters such as density, cosmic ray ionization rate, extinction, metal abundance, initial elemental abundance and temperature have been studied in detail (e.g. see for example: de Jong et al., 1980; Mitchell et al., 1978; Prasad and Huntress, 1980; Graedel et al., 1982), the bulk of this discussion concerning variable parameters is focused primarily on those which effect grain composition, with the effects on the gas phase described only briefly. First, density and ultraviolet flux within the cloud are considered: mantle composition will vary because of the different timescales for accretion and ejection and the timescale for the photodestruction of gas phase molecules depends strongly on extinction. This is followed by a discussion of how particular assumptions concerning grain chemistry effect grain mantle composition, with some attention given to the role of the surface reaction:

$$CO + O \rightarrow CO_2 \quad (24)$$

and the question of whether or not molecules are released directly upon formation on a surface. Finally how the grain composition depends upon elemental abundances is also investigated.

3.3.1. n_H and A_v dependence

Since the accretion rate is proportional to the density, an increase or decrease of n_H will change the influence grains have on the chemistry. Grain mantle composition evolution for different pairs of values of n_H and A_v, choosen to be representative of different regions outside of cloud cores are shown in Figs. 7–10.

In the low density, low extinction region, H_2O is always the major constituent of grain mantles. Although the overall trends remain similar to those of the standard case, it is remarkable to note the more significant difference appearing between the gas and the solid phase as illustrated in Table 6. This is due to the fact that molecules such as H_2O and NH_3 are quickly photodissociated in the gas phase and their abundances in the grains do not reflect their abundances in the gas phase. Because, in this situation, atomic hydrogen remains abundant and because oxygen remains atomic in the gas phase, water is easily formed on the grain surface. Nitrogen and carbon in the gas phase evolve more slowly. Although the carbon is transformed to CO through gas phase reactions, atomic carbon remains comparable with CO for 10^6 years. The presence of a relatively high level of atomic carbon

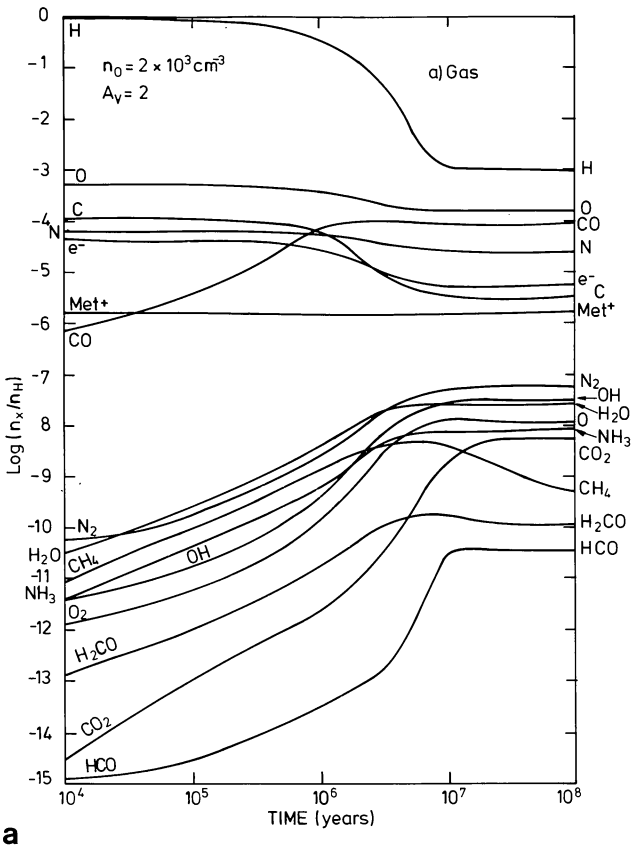

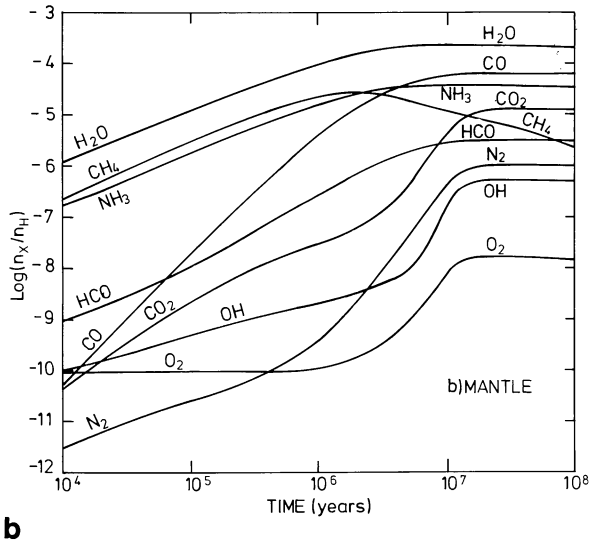

Fig. 7a and b. Time evolution of fractional gas phase **a** and solid phase **b** abundances for $n_0 = 2\ 10^3\,cm^{-3}$ and $A_v = 2$. Not all species are shown

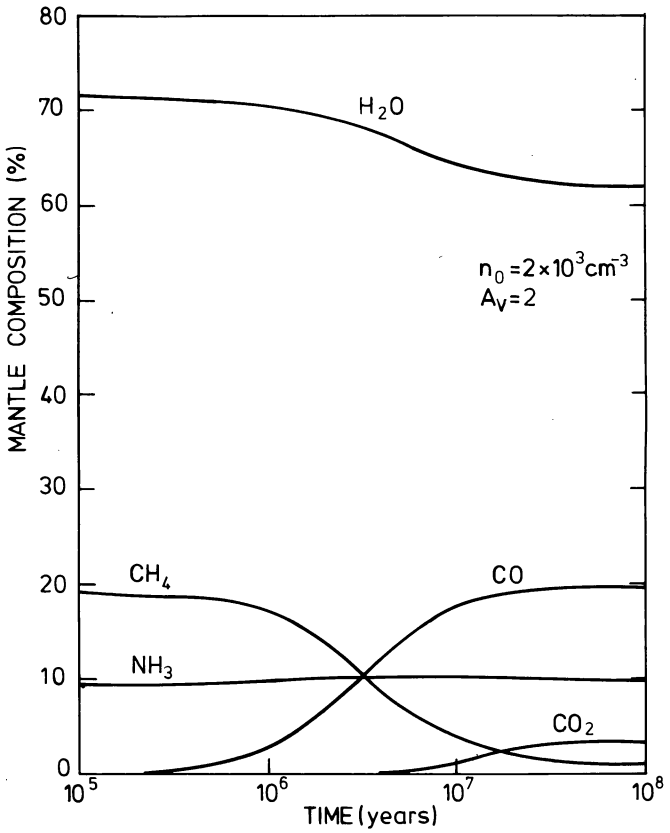

Fig. 8. Time evolution of the mantle composition (%) in the low density, low extinction region described in Fig. 7a and b. Not all species are shown

maintains an appreciable amount of methane in the grain mantles, 10%, until 3 10^6 years; a small fraction of CH_4 (~2%) remaining at equilibrium. Carbon monoxide, made from gas phase reactions is accreted on the grains and only a small fraction of this carbon monoxide can be transformed via surface reactions to CO_2 if reaction 24 occurs. However, it is interesting to note that, at the grain surface, atomic oxygen reacts primarily with H to form H_2O so that the reaction with CO is only marginal; the CO_2 content of the mantle does not exceed 4% when reaction 24 is included. The nitrogen behaves similarly to oxygen: for $A_v = 2$, its photodissociation in the gas phase is rapid and its primary reaction at the grain surface leads to the formation of ammonia. NH_3 remains in the mantle to the significant level of 10% because it is made continuously on the grain surface. Finally it is to be noted that for a low value of extinction, molecular oxygen and nitrogen are not abundant in the gas phase because of their relatively high photodissociation rates; they are also absent from the mantles because surface reactions of O and N with abundant H atoms form H_2O and NH_3. For such an extinction, it is also expected that chemical modification of the grain mantles from UV bombardment will be important. It is well known however that the photodissociation rates of molecules in the solid phase are much slower than those in the gas phase because of cage effects which favor recombination of photolysis products back to the original molecule (see, for example, Bass and Broida, 1960). Thus, the trends described above will remain even if photolysis of mantles is taken into account.

In the opposite situation of high density and high extinction, the situation changes drastically as shown in Figs. 9 and 10 and Table 7. Gas phase evolution is faster for short timescales and atomic carbon is very quickly removed, forming CO in less than 3 10^5 years. Other species show more complicated time evolution and the time for equilibrium becomes extremely long, on the order of 5 10^7 years. Abundances show a quasi-equilibrium behavior between 10^6 and 10^7 years, followed by notable changes for a few

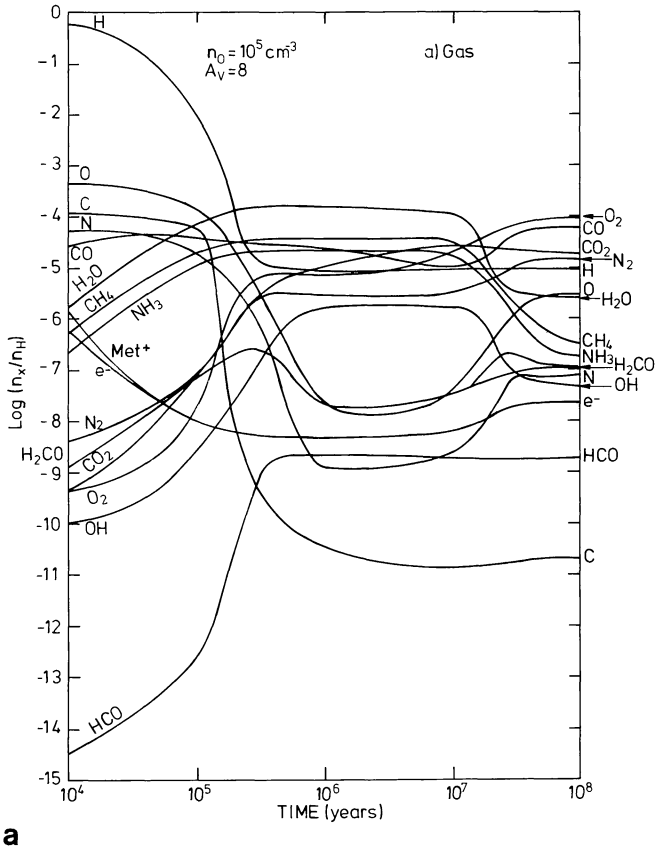

a

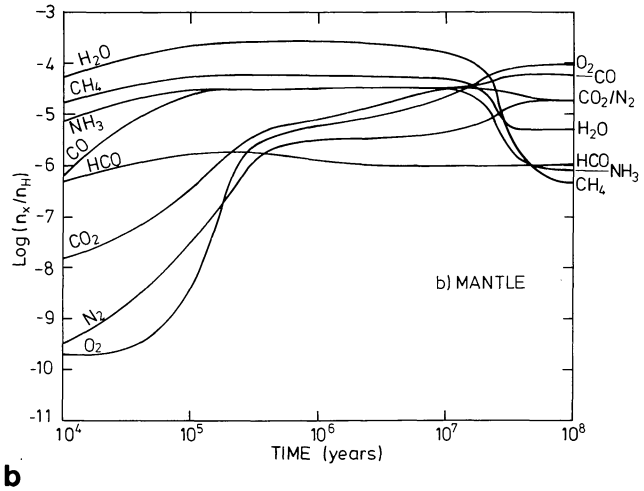

b

Fig. 9a and b. Same as Fig. 7 but for $n_0 = 10^5\,\mathrm{cm}^{-3}$ and $A_v = 8$

species between 10^7 and 10^8 years. Although the situation appears extremely complicated a few trends can be explained in terms of the duality of the chemistry involving gas and grains: for short timescales, this chemistry is entirely dominated by grain processes so that molecules like H_2O, CH_4, and NH_3 are abundantly made on grains and are also present in the gas phase. Although in this case the atomic hydrogen is quickly transferred to H_2 and disappears from the gas phase, slowing down the formation rates of saturated molecules as H_2O, CH_4, and NH_3 drops considerably, these molecules survive longer than in the previous case of lower

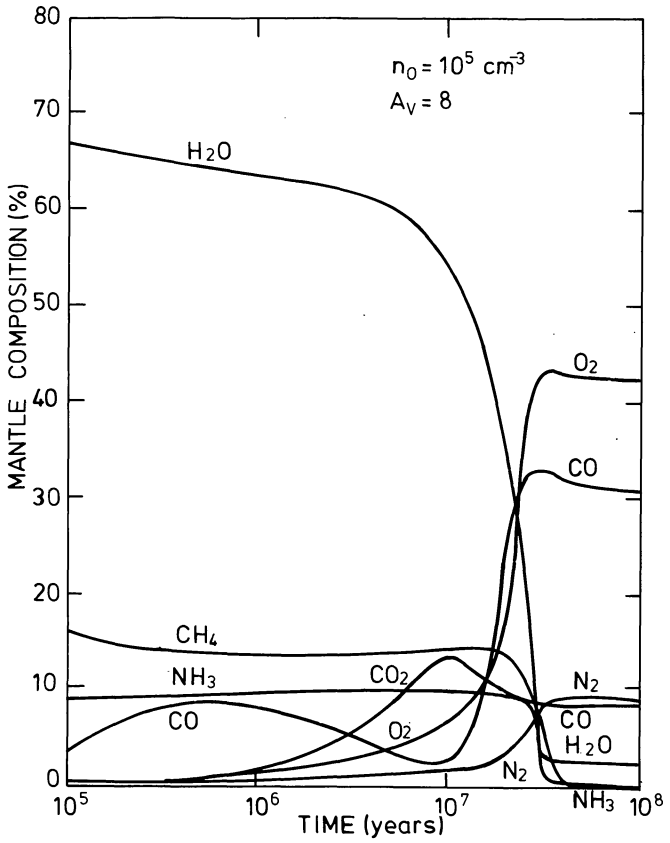

Fig. 10. Time evolution of the mantle composition (%) in the high density, high extinction region described in Fig. 9a and b. Not all species are shown

Table 6. Comparison of the abundances of different molecules present in the gas and the solid phase at 10^5, 10^6, and 10^7 years for $n_0 = 2\ 10^3$ and $A_v = 2$

Time (years)	Species	Gas phase	Solid phase
10^5	H_2O	$2.9\ 10^{-10}$	$1.1\ 10^{-5}$
	CH_4	$1.1\ 10^{-10}$	$3.0\ 10^{-6}$
	NH_3	$4.6\ 10^{-11}$	$1.5\ 10^{-6}$
	O_2	$6.7\ 10^{-12}$	$9.6\ 10^{-11}$
	N_2	$2.1\ 10^{-10}$	$2.6\ 10^{-11}$
	CO	$2.1\ 10^{-10}$	$2.6\ 10^{-11}$
	CO	$3.7\ 10^{-6}$	$2.0\ 10^{-3}$
	CO_2	$1.3\ 10^{-13}$	$2.4\ 10^{-9}$
10^6	H_2O	$3.2\ 10^{-9}$	$9.0\ 10^{-5}$
	CH_4	$1.2\ 10^{-9}$	$2.2\ 10^{-5}$
	NH_3	$5.5\ 10^{-10}$	$1.3\ 10^{-5}$
	O_2	$1.1\ 10^{-10}$	$8.9\ 10^{-11}$
	N_2	$2.5\ 10^{-9}$	$3.4\ 10^{-10}$
	CO	$4.7\ 10^{-5}$	$3.4\ 10^{-6}$
	CO_2	$2.3\ 10^{-12}$	$2.8\ 10^{-8}$
10^7	H_2O	$2.4\ 10^{-8}$	$2.1\ 10^{-4}$
	CH_4	$3.0\ 10^{-9}$	$1.3\ 10^{-5}$
	NH_3	$6.5\ 10^{-9}$	$3.6\ 10^{-5}$
	O_2	$1.2\ 10^{-8}$	$8.0\ 10^{-9}$
	N_2	$4.7\ 10^{-8}$	$3.4\ 10^{-7}$
	CO	$7.3\ 10^{-5}$	$5.8\ 10^{-5}$
	CO_2	$1.9\ 10^{-9}$	$4.1\ 10^{-6}$

Table 7. Comparison of the abundances of different molecules present in the gas and the solid phase at 10^5, 10^6, 10^7, and 10^8 years for $n_0 = 10^5$ and $A_v = 8$

Time (years)	Species	Gas phase	Solid phase
10^5	H_2O	$8.0\ 10^{-5}$	$2.2\ 10^{-4}$
	CH_4	$2.0\ 10^{-5}$	$5.4\ 10^{-5}$
	NH_3	$1.2\ 10^{-5}$	$3.3\ 10^{-5}$
	O_2	$1.5\ 10^{-8}$	$3.0\ 10^{-9}$
	N_2	$6.1\ 10^{-8}$	$2.2\ 10^{-8}$
	CO	$3.9\ 10^{-5}$	$2.4\ 10^{-5}$
	CO_2	$7.3\ 10^{-8}$	$3.0\ 10^{-7}$
10^6	H_2O	$1.6\ 10^{-4}$	$2.2\ 10^{-4}$
	CH_4	$3.5\ 10^{-5}$	$5.0\ 10^{-5}$
	NH_3	$1.9\ 10^{-5}$	$2.9\ 10^{-5}$
	O_2	$6.6\ 10^{-6}$	$6.5\ 10^{-6}$
	N_2	$2.6\ 10^{-6}$	$2.9\ 10^{-6}$
	CO	$2.6\ 10^{-5}$	$2.8\ 10^{-5}$
	CO_2	$2.4\ 10^{-6}$	$7.4\ 10^{-6}$
10^7	H_2O	$1.2\ 10^{-4}$	$1.6\ 10^{-4}$
	CH_4	$3.0\ 10^{-5}$	$4.4\ 10^{-5}$
	NH_3	$1.8\ 10^{-5}$	$2.7\ 10^{-5}$
	O_2	$1.9\ 10^{-5}$	$1.9\ 10^{-5}$
	N_2	$3.7\ 10^{-6}$	$4.0\ 10^{-6}$
	CO	$9.5\ 10^{-6}$	$9.2\ 10^{-6}$
	CO_2	$3.3\ 10^{-5}$	$2.7\ 10^{-5}$
10^8	H_2O	$2.4\ 10^{-6}$	$5.3\ 10^{-6}$
	CH_4	$4.0\ 10^{-7}$	$6.6\ 10^{-7}$
	NH_3	$3.0\ 10^{-7}$	$6.0\ 10^{-7}$
	O_2	$7.4\ 10^{-5}$	$8.0\ 10^{-5}$
	N_2	$1.5\ 10^{-5}$	$1.5\ 10^{-5}$
	CO	$5.5\ 10^{-5}$	$5.6\ 10^{-5}$
	CO_2	$2.0\ 10^{-5}$	$2.7\ 10^{-5}$

extinction. Consequently they remain longer in the gas phase as well as in the mantle. In the gas phase their evolution is extremely slow. The same trend is observed for the atoms; although C, O, and N are quickly removed from the gas phase, CH_4, H_2O, and NH_3 are made efficiently at short times and will remain abundant in both phases. A quasi-equilibrium is then reached and continues for a long time until gas phase reactions start re-arranging the chemistry. Stable molecules as O_2 and N_2 are produced and consequently water disappears from the mantle because most of the oxygen is locked up in O_2. This is also the case for ammonia where nitrogen is eventually trapped in N_2. This latter case has already been observed in the standard model where it was noted that N_2 was present in the mantle at the expense of ammonia (Fig. 6). The transformation of atomic to molecular oxygen also prevents the formation of much CO_2; CO remaining one of the most abundant molecule in the mantle. From a water rich mantle, evolution leads to a molecular oxygen, carbon monoxide rich one, where water is no longer dominant (only 3%). This trend is also obtained at somewhat lower values of density and extinction for the evolution of the predominant nitrogen containing species proceeding from atomic nitrogen to NH_3 then to N_2.

3.3.2. Dependence on initial elemental abundances

As is well known, different equilibria can be achieved for different initial elemental abundances. In this section, the role a change in the elemental abundance has on the grain mantle composition is investigated. The data for these initial abundances, listed in Table 8, are taken from Tielens and Hagen (1982). The four different initial abundances have been used with the standard case conditions. Time evolution of mantle compositions are shown in Fig. 11a–d where 11b, corresponding to the elemental abundances observed in ξ Oph, has already been shown in Fig. 6 for the standard model. Equilibrium values are listed in Table 9 but the fact that a time of $5\ 10^6$ years is required to attain this equilibrium makes it more useful to compare the time evolution given in Fig. 11.

Table 8. Elemental abundances relative to hydrogen used to calculate mantle compositions illustrated in Fig. 11a–d. Table adopted from Tielens and Hagen (1982)

Elements	Cosmic	ξ Oph	*o* Per	ζ Per
C	$3.98\ 10^{-4}$	$1.58\ 10^{-4}$	$3.98\ 10^{-4}$	$2.88\ 10^{-4}$
N	$1.00\ 10^{-4}$	$6.31\ 10^{-5}$	$3.16\ 10^{-6}$	$5.82\ 10^{-4}$
O	$6.31\ 10^{-4}$	$5.01\ 10^{-4}$	$5.25\ 10^{-4}$	$6.31\ 10^{-4}$
Met	$3.2\ 10^{-5}$	$1.5\ 10^{-6}$	$2.5\ 10^{-6}$	$3.2\ 10^{-6}$
O/C	1.6	3.2	1.3	2.2

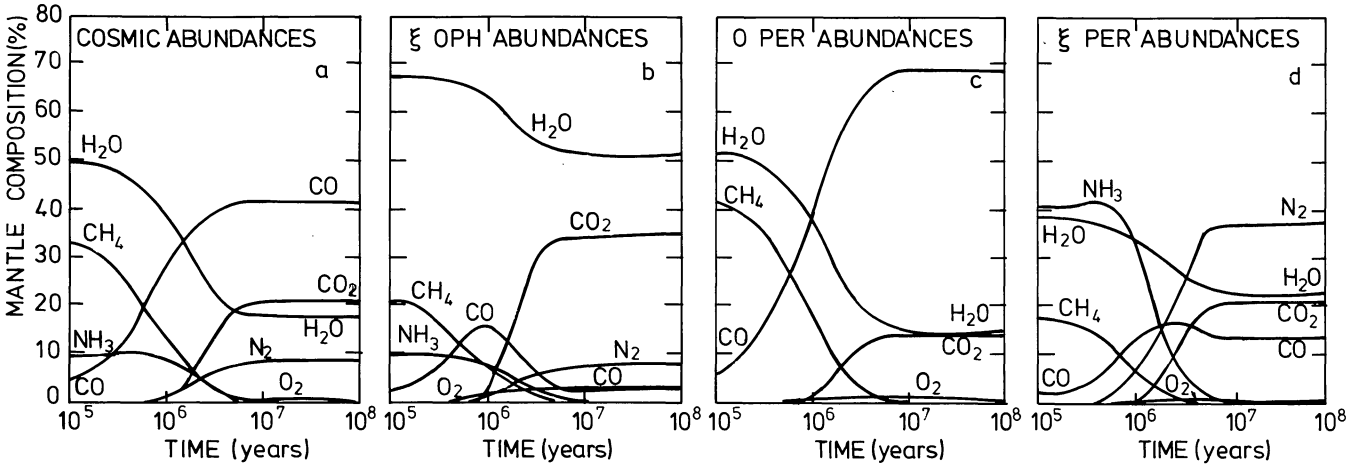

Fig. 11a–d. Time evolution of the mantle composition (%) for four different initial elemental abundances (see Table 8 and text). Not all species are shown

Table 9. Mantle composition (%) at equilibium for different conditions of abundances (see Fig. 11a–d)

Elements	Cosmic	ξ Oph	*o* Per	ζ Per
H_2O	18	52	15	22
CO	42	3	68	13
CH_4	–	–	–	–
NH_3	1	–	–	–
CO_2	21	34	14	21
O_2	2	2	2	1
N_2	9	8	–	33

As obvious from this figure, while different starting abundances lead to different mantle compositions, the general trend in the chemistry remains similar: H_2O, CH_4, and NH_3 are efficiently made at short times; other molecules such as CO, CO_2, N_2, and O_2 appear later. It is to be noted that in the standard model, with ξ Oph elemental abundances, a high concentration of H_2O remains in the mantle throughout the cloud lifetime. This is due to the fact that for this case, the O/C ratio has the highest value and consequently, atomic oxygen reacts primarily with atomic hydrogen to form H_2O at all times. For the other cases, H_2O is less abundant and a more important fraction of the mantle is made of CO at later stages. In the case of *o* Per, although the O/C ratio is smaller, CH_4 disappears from the mantle because of the preferential conversion of atomic carbon to CO. For a ratio O/C less than unity, all the atomic oxygen will probably be locked up in CO completely eliminating H_2O from the mantle and carbon rich mantles would then form, containing mostly CH_4. However, owing to its peculiarity, this case is not likely and hat not been considered here. When nitrogen is abundant (ζ Per abundances), ammonia is dominant at early times but eventually transformed to the stable N_2 molecule. With two exceptions, the trends described above are in good qualitative agreement with the results described by Tielens and Hagen (1982). It is to be noted however that formaldehyde is not abundant in our model since we have not included the reaction $H + HCO \rightarrow H_2CO$ for the reasons discussed in Sect. 2.2.2. Another difference is that, although the reaction of CO with atomic oxygen at the grain surface is allowed in our model, the carbon dioxide concentration in the mantle remains comparatively lower than that described by Tielens and Hagen due to the fact that we used a slower reaction rate for this reaction.

4. Comparison with observations

As emphasized by Graedel et al. (1982), comparison of results from chemical models with observations is not trivial. Our model is oversimplified, describing the chemistry at one point defined by the local density and visual extinction and encompassing only a limited set of reactions and species, without taking into account inhomogeneities, motions such as turbulence and temperature gradients. Moreover, the interpretation of the observations in terms of extraction of molecular abundances involves modeling the physical object by including, for example, radiation transfer, thermal excitation mechanisms and spectral resolution, each of which introduce uncertainties in the abundance determination. Because we have presented a model in which not only the gas phase compositions are calculated, each state will be compared with observations separately, starting with the gas. For the solid phase, the infrared spectroscopic characteristics of the calculated mantles have been measured in the laboratory and are compared with infrared observations.

4.1. Gas phase

To discuss the gas phase, we adopt the technique used by Graedel et al. (1982) who compared their results with a range of observations. References for the observations and abundances of these different molecules are given in detail in their paper. We have chosen to compare similarly, and for the same molecules, the results given by our standard model at 10^5, 10^6, and 10^7 years, such an approach being justified by the fact that it would be misleading to compare only equilibrium values to multiple observations where different conditions (e.g. cloud ages, geometry etc.) prevail. Moreover, for our standard model, at 10^7 years, equilibrium is reached and no further evolution takes place.

Figure 12, similar to Fig. 17 in Graedel et al. (1982), gives the comparison of the model; the following points are worth emphasizing.

CO and OH abundances are well predicted. As previously mentioned, atomic carbon is efficiently transferred to CO and its abundance is extremely low in a cold dark cloud. This is also true for other carbon bearing species such as H_2CO and CH. Although high column densities of neutral carbon have been measured in certain clouds (Phillips et al., 1980), as with previous time dependent calculations, carbon atoms are only abundant at very short times of evolution in the standard model. High

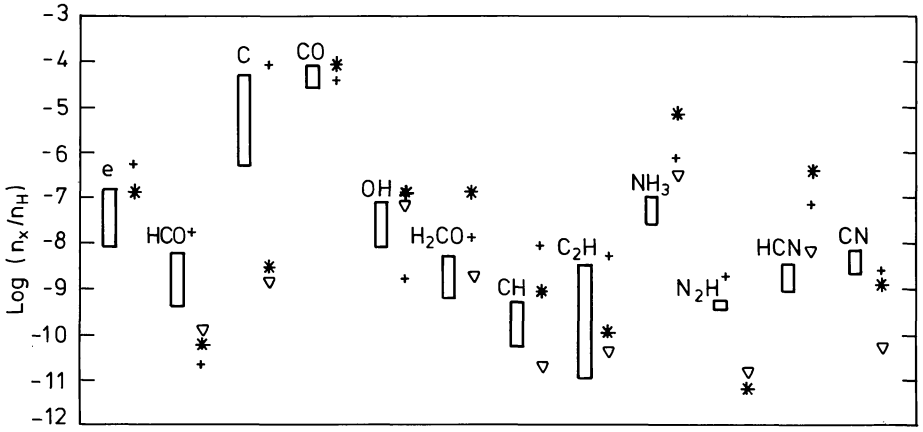

Fig. 12. Comparison of the standard model gas phase abundances with observations ($n_0 = 2\ 10^4$, $A_v = 4$). Calculated abundances are plotted at 10^5(+), 10^6(*) and 10^7(▽) years where equilibrium is reached. Values from observations as well as figure presentation are taken from Graedel et al. (1982). When data for 10^7 years is not indicated, values at 10^6 years are close to equilibrium

fractional abundance at longer times of carbon can be obtained only when a low value of extinction is used ($A_v \lesssim 2$) a value for which other molecules (CO, H_2CO, NH_3, H_2O) become extremely underabundant.

The electron abundance is rather low, in spite of the fact that a high metal abundance has been used. As already discussed, this low electron abundance follows naturally when grain charge is taken into account by the neutralization process described by Umebayashi and Nakano (1980). Recent work by Tielens and Hollenbach (1984) shows that the observed neutral carbon column densities can be explained by emission from the optically thin edge of the clouds where it has been measured.

Our model predicts reasonable amounts of amonia. NH_3 is made primarily on grains and, although the controversial gas phase reaction $H_3^+ + N \rightarrow NH_2^+ + H$, has not been included, the observed values for the abundance of NH_3 can be reproduced in reasonable agreement.

Although it should be possible to derive cloud ages from time dependent chemistry, the wide variations over the measured abundances make the determination of cloud ages very difficult. However, the strong time dependence of carbon bearing species such as H_2CO shows that cloud ages less than $5\ 10^5$ years are unlikely because carbon is not in CO before that time and at later stages, more than $3\ 10^6$ years, the abundance of H_2CO drops to a somewhat lower value. However, in this model, we have not taken into account the effect of UV photolysis of grain mantles which modify the composition of the mantles and hence the gas phase composition.

4.2. Solid phase

Mid infrared spectroscopy (2–20 microns) is one of the most direct ways to identify molecules adsorbed on grains in interstellar clouds. Broad absorption features appear superimposed on the continuum of many infrared sources observed in dense regions of dust. The width of these bands shows clearly that they are due to the presence of solid material (see for example Allamandola, 1984; Willner, 1984). While it is not presently possible to interpret the complete infrared spectrum in a quantitative way, much insight in the grain composition can be gained by comparing interstellar spectra with laboratory spectra of mixtures predicted by the model calculations described here in an analogous fashion to the comparison made by Tielens and Hagen (1982), with emphasis placed on band shape, position and the identification of a carrier of each band.

Two different compositions have been selected as representative of different types of calculated mantles. Type 1 is a water rich mantle, with H_2O representing 60 % of the sample, the other constituents being CO, NH_3, and CH_4; type 2 is rich in oxygen, carbon monoxide and water, with water comprising only about 25 % of the sample and NH_3, CH_4, and N_2 present as minor constituents. The spectra with the exact composition of the mixtures are shown in Fig. 13. Type 1 (a in the figure) is derived from the mantle composition at 10^6 years calculated in the standard case and type 2 represents the equilibrium composition calculated for the high extinction case ($A_v = 8$) in which most of the oxygen remains trapped in O_2 (see Figs. 6 and 10). Carbon dioxide

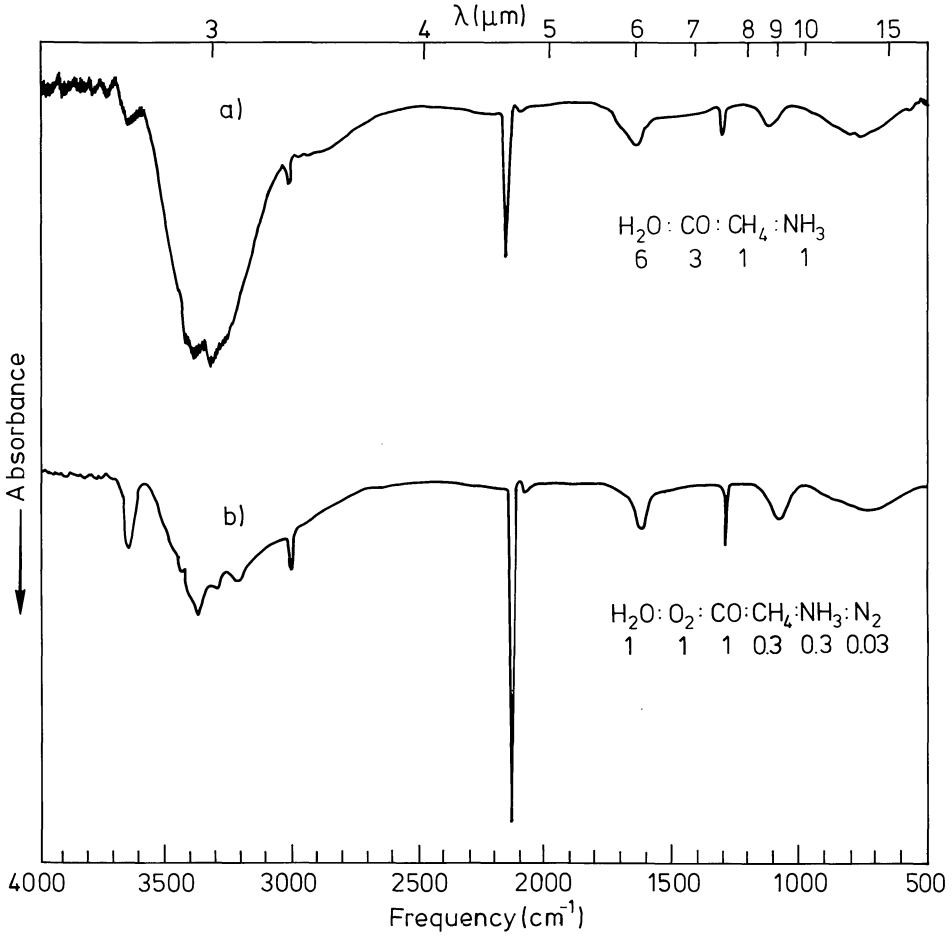

Fig. 13. Infrared spectra of **a** water rich and **b** oxygen, carbon monoxide rich mixtures corresponding roughly to the standard model composition at about $2\ 10^6$ years (see Figs. 5b and 6) and the $n_0 = 10^5$, $A_v = 8$ model at about $5\ 10^7$ years (see Figs. 9b and 10). Absorbance is given in arbitrary units

has not been included due to uncertainty in the rate of the surface reaction $CO + O \rightarrow CO_2$. Since this reaction is by far the most important channel for CO_2 formation, carbon will be locked up either in CO or CO_2 depending on this reaction rate. For high values of extinction, the oxygen is molecular and CO_2 is not very abundant whereas for low values of extinction oxygen is trapped in H_2O and CO_2 is also not very abundant. The infrared feature produced by CO and CO_2 will be friefly discussed followed by a comparison with the interstellar features. Moreover, because CO_2 is an important product in the UV photolysis of the mantles, a more thorough discussion will be given in Paper II.

H_2O. The spectrum of water in laboratory and interstellar ices is discussed in great detail by Hagen et al. (1983). While the features due to water are prominent in both spectra, they vary somewhat with the water concentration; the greatest changes occurring in the 3700–3000 cm^{-1} (2.7–3.3 microns) range. At the H_2O concentration in mixture 1 (60 %), most of the molecules are hydrogen bonded, forming amorphous H_2O ice, giving rise to the well known, broad 3.08 μm band. In mixture 2 (25 % H_2O), bands due to isolated and simple multimers (dimers, trimers) of H_2O appear as well and give rise to discrete bands (Van Thiel et al., 1957). There is a qualitative difference between the interstellar spectra associated with less dense region and these with more dense regions. The 3.1 μm interstellar band measured toward IR sources obscured by dense material is prominent with an appearance threshold lying in the range $A_v = 5 - 15$ (Whittet et al., 1983), while it is apparently not present towards objects obscured by diffuse material. Thus, the calculations described here for the case $A_v = 2, n_H = 2\ 10^3\ cm^{-3}$ do not reproduce the observations, presumably because the model does not attempt to take the effects of photodesorption and photochemical processing fully into account. However, it is to be noted that in the Taurus cloud stars, the appearance threshold for the ice band is particularly low ($A_v \sim 3.6$) as shown by Whittet et al. (1983) and Goebel (1983). There is no substantial change in the broad librational band which peaks between 770 and 740 cm^{-1} (13 to 13.5 μm) in these mixtures, broadened and shifted from the 830 cm^{-1} (12 μm) position in amorphous water. As pointed by Hagen and Tielens (1982) this shift and broadening makes it difficult to detect in interstellar spectra which, due to overlap with the strong telluric CO_2 bands cut off at about 700 cm^{-1} (14 μm). In any case *this band can not be confused with or hidden by the silicate band* which is centered at about 1030 cm^{-1} and is sharper. A search for this librational band of H_2O should be made between 12 and 17 microns, a region accessible only, to the IRAS satellite. H_2O also absorbs at 1665 cm^{-1} (6.0 μm), a band which is much less sensitive to environmental effects, making it *the most reliable* region in which to probe the amount of interstellar, solid state H_2O in spite of problems associated with blending.

CO and CO_2. Carbon monoxide generally absorbs between 2130 and 2145 cm^{-1} (4.69 – 4.66 microns) depending on its concentration and the nature of the other ice constituents. Carbon dioxide absorbs very strongly at 2350 cm^{-1} (4.26 μm) and moderately at 670 cm^{-1} (4.9 μm). Solid CO has been detected with good reliability to allow column density determination in the sources reported by Lacy et al. (1984) as well as in several others (Geballe, private communication). Carbon dioxide detection at these wavelengths is not possible, even with airborne telescopes, due to its large scale height in the Earth's atmosphere and can only be searched for from space.

CH_4. Methane is the simplest saturated hydrocarbon and, as such, is in a class by itself chemically and spectroscopically with a C—H stretching frequency near 3010 cm^{-1} (3.3 μm) and deformation frequency near 1305 cm^{-1} (7.66 μm). Virtually all other saturated hydrocarbons possess corresponding frequencies in the ranges 2960–2850 cm^{-1} (3.4–3.5 μm) and 1465–1360 cm^{-1} (6.8–7.4 μm) respectively. Although interstellar absorptions at 3010 and 1305 cm^{-1} have not been detected, the methane bands tend to be narrower than the other solid state features and fall in difficult spectral regions. The band at 3010 cm^{-1} is easily obscured by the water band, requiring not only moderate resolution ($\lambda/\Delta\lambda = 1500$) but also an extremely good signal-to-noise ratio. This latter requirement is difficult to realize because of overlap with the atmospheric methane bands. The 1305 cm^{-1} band does not suffer from the threat of overlap by other much stronger bands, but does fall in a region requiring good signal to noise airborne observations. The use of the moderate resolution multi-element, faint object gratin spectrometer (FOGS) developed by Witteborn and Bregman (1984) at the NASA Ames Research Center, may make it possible to detect this band.

NH_3. Ammonia gives rise to significant absorption centered at 3380 cm^{-1} (2.96 μm), 1630 cm^{-1} (6.13 μm) and about 1100 cm^{-1} (9.7 μm) as well as producing a long wavelength wing on the 3.08 μm H_2O ice band. Absorption corresponding to all but the 9.1 μm band, not distinguishable due to overlap with the 10 μm silicate band, have been measured in the interstellar medium, with the NH_3/H_2O ratio still quite uncertain (Knacke et al., 1982; Greenberg et al., 1983; Tielens et al., 1984).

O_2, N_2. Oxygen and nitrogen, the other molecules used in these mixtures are not infrared active and impossible to probe in the infrared.

Table 10 lists the interstellar bands as well as the molecules considered here which could contribute to them in order of decreasing importance. While the interstellar bands are generally broader than those shown in Fig. 11a and b, the fact that these calculated mixtures, the result of an admittedly oversimplified calculation, can account for the bulk of the interstellar bands is not only encouraging, but also indicative of the kind of changes required to improve the match. Further energetic processing is needed to create the new molecular bands required to reproduce the other interstellar bands which occur at 3.4, 4.67, and 6.8 μm as well as broaden the 6.0 μm feature by the required amount. While a full discussion of the chemistry and spectroscopy of these mixtures

Table 10. List of interstellar absorption bands attributable to grain mantle consituents and the molecules which contribute to these bands postulated by the model calculations

Interstellar bands	Postulated band carrier
2.98	NH_3, H_2O
3.08	H_2O
3.08 long λ wing	H_2O—NH_3
3.4 [a]	–
4.61 [a]	–
4.67	CO
6.0	H_2O, NH_3
6.8 [a]	

[a] Bands at these frequencies can be produced by UV photolysis, see text and Paper II

as they undergo ultraviolet photoprocessing is beyond the scope of this paper, it is important to point out that photolysis produces absorptions at 3.4 and 6.8 μm due to the production of saturated hydrobarbons more complex than CH_4 and at 4.67 μm due to the production of CN, in either the cyano ($-C\equiv N$) or isocyano ($C\equiv N-$) form, in a way similar to and consistent with the experiments described by Lacy et al. (1984). Tielens et al. (1984) discuss the spectroscopic variations in the 5–8 μm region. It is also relevant to note that, upon photolysis of mixture 2, CO is readily converted to CO_2, with the 2350 and 660 cm^{-1} CO_2 bands growing at the expense of the 2140 cm^{-1} CO band. The spectroscopic and chemical effects induced by UV photolysis, together with an analysis of the integrated absorbance of these and other molecules and comparison with interstellar spectra form the subject of Paper II.

5. Conclusion

For the first time, a time-dependent model is described which includes the role of grains in the production of molecules in dense clouds including ion-molecule gas phase chemistry. The approach provides information regarding the coupling between the two phases. Although the coupling between the two chemistries is extremely strong, these two different domains maintain their own identity; while H_2O, CH_4, and NH_3 are made efficiently, with a high production rate on grains and released back to the gas phase, the gas phase is essentially responsible for the formation of CO, a very stable molecule which, may or may not react on grains with atomic oxygen and form or not CO_2. Consequently, gaseous carbon largely remains in CO in the gas phase although an appreciable amount of CO_2 might also be present if oxygen is available in atomic form. For high extinction values, this is not the case and CO_2 is not abundant.

As predicted by van de Hulst (1949), ices of H_2O, CH_4 and NH_3 are present but only at short times when hydrogen is present in atomic form. Only H_2O will remain abundant at all cloud ages provided that oxygen remains atomic ($A_v \leqq 4$). Methane and ammonia show strong time dependence because carbon and nitrogen are converted to the stable molecules CO and N_2. Diffusion controlled slower reactions on the grain surface become important only when atomic hydrogen has been converted to H_2, producing molecules such as O_2, N_2, CO and perhaps CO_2 which eventually become abundant mantle constituents. Unfortunately, of this list, only CO can presently be observable and has been observed. In oxygen rich mantles however a different chemistry can be initiated by UV photolysis and is expected to yield somewhat different products than those produced by the photochemistry of water rich mantles. Some of the photoproducts can be observed in the infrared region of the spectrum. Such processes which modify the results presented here form the subject of Paper II.

The composition of the mantle does not necessarily reflect the composition of the gas phase, especially in regions with lower A_v values where the photodestruction rates for gas phase molecules are high. Accretion on grains is an important part of the chemistry as shown by the differences in calculated grain compositions which result if mantles are formed by accretion alone or formed by taking all the processes discussed here into account. Accretion and surface reactions cannot be ignored in model calculations of interstellar chemistry.

Acknowledgements. It is a pleasure to thank Dr. A.G.G.M. Tielens for his help at the beginning of this work and particularly in providing his computer code for the initial gas phase chemistry and a critical reading of an earlier version of the manuscript. We thank Dr. Leo van IJzendoorn for many stimulating discussions and help in formulating the solid state reaction scheme.

References

Allen, M., Robinson, G.W.: 1975, *Astrophys. J.* **195,** 81
Allen, M., Robinson, G.W.: 1977, *Astrophys. J.* **212,** 396
Barlow, M.J.: 1978, *Monthly Notices Roy. Astron. Soc.* **183,** 397
Bass, A.M., Broida, H.P.: 1960, Formation and Trapping of Free Radicals, Academic Press, New York
Black, J.H., Dalgarno, A.: 1973, *Astrophys. Letters* **15,** 79
Black, J.H., Dalgarno, A.: 1977, *Astrophys. J. Suppl. Series* **34,** 405
Boer, K.S. de: 1981, *Astrophys. J.* **244,** 848
Boland, W.: 1982, Ph.D. Thesis, University of Amsterdam, The Netherlands
Boland, W., de Jong, T.: 1982, *Astrophys. J.* **261,** 110
Bourdon, E.B., Prince, R.H., Duley, W.W.: 1982, *Astrophys. J.* **260,** 909
Bult van de, C.E.P.M., Allamandola, L.J., Baas, F., Van IJzendoorn, L.J., Greenberg, J.M.: 1980, *J. Mol. Struct.* **61,** 235 and unpublished results
Burke, J.R., Hollenbach, D.J.: 1983, *Astrophys. J.* **265,** 223
Devienne, F.M.: 1953, *J. Phys. Radium* **14,** 257
Draine, B.T., Salpeter, E.E.: 1979, *Astrophys. J.* **231,** 438
Folman, H., Klein, R.: 1968, *Surf. Sci.* **11,** 430
Fournier, J., Deson, J., Vermeil, C., Pimentel, G.C.: 1979, *J. Chem. Phys.* **70,** 5726
Gammon, R.H.: 1978, *Chemical Eng. News* **56,** No. 41, 21
Goebel, J.H.: 1983, *Astrophys. J. Letters* **965,** L41
Graedel, T.E., Langer, W.D., Frerking, M.A.: 1982, *Astrophys. J. Suppl.* **48,** 321
Greenberg, L.T.: 1973, in *Interstellar Dust and Related Topics, IAU Symp.* No. **52,** eds. J.M. Greenberg, H.C., van de Hulst, Reidel, Dordrecht, p. 431
Greenberg, J.M.: 1974, *Astrophys. J.* **189,** L81
Greenberg, J.M.: 1977, in *Liège Astrophysical Symposium on Small Molecules*, June 1977, p. 555
Greenberg, J.M.: in *Cosmic Dust*, ed. J.A.M. McDonnell, Wiley, New York, p. 187
Greenberg, J.M.: 1979, in *Stars and Star Systems*, ed. B.E. Westerlund, Reidel, Dordrecht, p. 173
Greenberg, J.M., Yencha, A.: 1973, in *Interstellar Dust and Related Topics*, IAU *Symp.* No. **52,** eds. J.M. Greenberg, H.C. van de Hulst, p. 369
Greenberg, J.M., Van de Bult, C.E.P.M., Allamandola, L.J.: 1983, *J. Chem. Phys.* **87,** 4243
Grim, R., d'Hendecourt, L.B.: 1985, *Astron. Astrophys.* (in preparation)
Guélin, M., Langer, W.D., Wilson, R.W.: 1982, *Astron. Astrophys.* **107,** 107
Habing, J.H.: 1968, *Bull. Astron. Inst. Netherlands* **19,** 421
Hagen, W., Allamandola, L.J., Greenberg, J.M.: 1980, *Astron. Astrophys.* **86,** L3
Hagen, W., Tielens, A.G.G.M., Greenberg, J.M.: 1981, *Chem. Phys.* **56,** 367
Hagen, W., Tielens, A.G.G.M.: 1982, *Spectrochimica Acta* **38A,** 1089
Hagen, W., Tielens, A.G.G.M., Greenberg, J.M.: 1983, *Astron. Astrophys.* **117,** 132
Hale, B.N., Kiefer, J., Ward, C.A.: 1981, *J. Chem. Phys.* **75,** 1991

Hall, G., Watt, J.M.: 1976, Modern Numerical Methods for Ordinary Differential Equations, Clarendon Press, Oxford, England
Hallam, H.E.: 1973, in *Vibrational Spectroscopy of Trapped Species*, ed. H.E. Hallam, Wiley, London
d'Hendecourt, L.B., Allamandola, L.J., Baas, F., Greenberg, J.M.: 1982, *Astron. Astrophys.* **109,** L12
d'Hendecourt, L.B.: 1984, Ph. D. Thesis, University of Leiden, The Netherlands
Herbst, E., Klemperer, W.: 1973, *Astrophys. J.* **185,** 505
Hollenbach, D., Salpeter, E.E.: 1970, *J. Chem. Phys.* **53,** 79
Hollenbach, D., Salpeter, E.E.: 1971, *Astrophys. J.* **163,** 155
Hulst, H.C., van de: 1949, *Rech. str. Obs. Utrecht* **11,** Part 2
Iglesias, E.: 1977, *Astrophys. J.* **218,** 697
Jong, T.: 1972, Ph.D. Thesis, University of Leiden, The Netherlands
Jong, T., de, Kamijo, F.: 1973, *Astron. Astrophys.* **25,** 363
Jong, T. de, Dalgarno, A., Boland, W.: 1980, *Astron. Astrophys.* **91,** 68
Jura, M.: 1974, *Astrophys. J.* **191,** 375
Kessler, M.F., Phillips, J.P.: 1984, *Galactic and Extragalactic Infrared Spectroscopy*, eds. M.F. Kessler, J.P. Phillips, Reidel, Dordrecht
Knacke, R.F., McCorkle, S., Puetter, R.C., Erickson, E.F., Krätschmer, W.: 1982, *Astrophys. J.* **260,** 141
Lacy, J.H., Baas, F., Allamandola, L.J., Persson, S.E., McGregor, P.J., Landsdale, C.J., Geballe, T.R., van de Bult, C.E.P.M.: 1984, *Astrophys. J.* **276,** 533
Lander, J.J., Morrison, J.: 1964, *J. Appl. Phys.* **35,** 3593
Lee, T.J.: 1972, *Nature* **237,** 99
Léger, A., Klein, J., de Cheveigne, S., Guinet, C., Defourneau, D., Belin, M.: 1979, *Astron. Astrophys.* **79,** 256
Léger, A.: 1983, *Astron. Astrophys.* **123,** 271
Léger, A., Jura, M., Omont, A.: 1985, *Astron. Astrophys.* **144,** 147
Lugger, P.M., York, D.G., Blanchard, I., Morton, D.C.: 1978, *Astrophys. J.* **224,** 1059
McCarrol, B., Ehrlich, G.: 1963, *J. Chem. Phys.* **38,** 523
McCarrol, B., McKee, D.W.: 1971, *Carbon* **9,** 301
Mitchell, G.F., Ginsburg, J.L., Kuntz, P.J.: 1978, *Astrophys. J. Suppl.* **38,** 39
Mohammed, H.H., Fournier, J., Deson, J., Vermeil, C.: 1980, *Chem. Phys. Letters* **73,** 315
Morton, D.C.: 1974, *Astrophys. J.* **143,** L35
Nishi, N., Shinohara, H., Okuyama, T.: 1984, *J. Chem. Phys.* **80,** 3898
Oppenheimer, M., Dalgarno, A.: 1974, *Astrophys. J.* **192,** 29
Phillips, T.G., Huggins, P.K., Kuiper, T.B.H., Miller, R.E.: 1980, *Astrophys. J. Letters* **238,** L103
Prasad, S.S., Huntress, W.T.: 1980, *Astrophys. J. Suppl.* **43,** 1
Prasad, S.S., Tarafdar, S.P.: 1983, *Astrophys. J.* **267,** 603
Redhead, P.A., Hobson, J.B., Kornelsen, E.V.: 1968, in *The Physical Basis of Ultrahigh Vacuum*, Chapman and Hall, London
Salpeter, E.E.: 1971, in *Highlights of Astronomy*: *14th IAU General Assembly*, Reidel, Dordrecht, p. 429
Shinoda, T.: 1969, *Bull. Chem. Soc. Japan* **42,** 2815
Silk, J., Norman, C.A.: 1980, in *Interstellar Molecules*, IAU *Symp.* **87,** ed. B.H. Andrew, Reidel, Dordrecht, p. 165
Smardzewski, R.R.: 1978, *J. Chem. Phys.* **68,** 2878
Soifer, B.T., Puetter, R.C., Russell, R.W., Willner, S.P., Harvey, P.M., Gillett, F.C.: 1979, *Astrophys. J.* **232,** L53
Spitzer, L. Jr.: 1978, in *Physical Processes in the Interstellar Medium*, Wiley, New York
Tielens, A.G.G.M., Hagen, W.: 1982, *Astron. Astrophys.* **114,** 245
Tielens, A.G.G.M., Hollenbach, D.: 1984, Protostars and Planets II, Sponsored by the University of Arizona, January 1984
Tielens, A.G.G.M., Allamandola, L.J., Bregman, J., Goebel, J., d'Hendecourt, L.B., Witteborn, F.C.: 1984, *Astrophys. J.* **287,** 697
Trumpler, R.J.: 1930, *Publ. Astron. Soc. Pacific* **42,** 214
Tully, R.J.: 1980, *Adv. Chem. Phys.* **42,** 63
Turner, B.E.: 1974, *J. Roy. Astron. Soc. Canada* **68,** 55
Umebayashi, T., Nakano, T.: 1980, *Publ. Astron. Soc. Japan* **32,** 405
Van IJzendoorn, L.J., Allamandola, L.J., Baas, F., Greenberg, J.M.: 1983, *J. Chem. Phys.* **78,** 7019
Van IJzendoorn, L.J.: 1985, Ph. D. Thesis, University of Leiden, The Netherlands
Van Thiel, M., Becker, E.D., Pimentel, G.C.: 1957, *J. Chem. Phys.* **59,** 5199
Watson, W.D.: 1973, *Astrophys. J.* **182,** L69
Watson, W.D.: 1974, in *Atomic and Molecular Physics and the Interstellar Matter*, Les Houches Summer School, eds. R. Balian, P. Encrenaz, J. Lequeux, North-Holland, Amsterdam, 1975, p. 177
Watson, W.D., Salpeter, E.E.: 1972, *Astrophys. J.* **174,** 321
Watson, W.D.: 1984, in *Galactic and Extragalactic Infrared Spectroscopy*, eds. M.F. Kessler, J.P. Phillips, Reidel, Dordrecht, p. 69
Willner, S.P.: 1984, in *Galactic and Extragalactic Infrared Spectroscopy*, eds. M.F. Kessler, J.P. Phillips, Reidel, Dordrecht, p. 37
Whittet, D.C.B., Bode, H.F., Longmore, A.J., Baines, D.W.T., Evans, A.: 1983, *Nature* **303,** 318
Witteborn, F.C., Bregman, J.D.: 1984, in *Proc. 28th Annual International Technology Symposium*, SPIE